UNIVERSITA' DEGLI STUDI DI PADOVA

FACOLTA' DI INGEGNERIA

Corso di Laurea Magistrale in Ingegneria Civile – Geotecnica

Dissertation

The Use of Seismic Waves for Geotechnical Characterization of Residual Soil from Porto

Davide Besenzon

October 2013

Supervised by
Prof. Paolo Simonini
Co-supervised by
Prof. Antonio Viana da Fonseca

To my parents and my friend Massimo

Acknowledgements

I'm extremely pleased for the high number of people who collaborated with me and especially those with whom I shared my time during my dissertation. For sure I will not be able to mention them all, but everyone has my sincere gratitude.

First of all I would like to thank my supervisor, Professor Paolo Simonini, for the idea and first guidelines of this work and, for being there to answer all my questions. My special thanks go also to my co-supervisor, Professor António Viana da Fonseca, for his continuous support and advice during all this time and, especially, in the critical moments, no words can express enough my gratitude to him. I feel lucky to have worked with him.

I wish also to thank all the staff of the Geotechnical Laboratory of FEUP, Mr. Armando Pinto, Claudia and Daniela who gave me great help.

Moreover, this work would not be possible without the help of my lab partners namely Fabrizio, Marisa, Marco, Helena and Miguel., Miguel.

Finally, I cannot forget my family and friends who have supported me in all times.

1
INTRODUCTION

This dissertation deals with soil characterization methods based on laboratory tests applied to geotechnical engineering purposes. At first, an overview of the properties of residual soil from Porto and seismic waves is presented, finally laboratory tests carried out and the role that the sismic waves took over in these tests are shown. In the last few decades, it has been recognized the Increasing role of seismic measurements in geotechnical engineering. The quality of the samples used in the laboratory is one of the most relevant aspects for deducing reliable geotechnical parameters. The classical techniques for evaluating the quality of these samples, including visual inspection of the fabric, measuring the volumetric variation etc, can be used on soils of sedimentary origin, but they do not adapt completely to the residual soils. One of the most interesting techniques for evaluating the quality of the samples is the comparison of the speeds of the seismic waves in situ and in the laboratory.

Among the most important advances that were made in the field of geotechnical engineering, in the last few decades, one of the most relevant advances was made in the study of the model of soil stiffness. Traditionally, geotechnical engineers have dedicated a lot of time and energy to the research of imperial correlations between the model of Young E1 of the soil and other parameters deduced in situ. The objective of this work is also to show the degradation of the stiffness model of the soil that is widespread in the Porto region.

2
STATE OF ART

2.1 RESIDUAL SOIL OF PORTO

2.1.1. INTRODUCTION TO THE ORIGIN AND FORMATION OF RESIDUAL SOIL

Residual soils are found in many parts of the world. Like other soils, they are used extensively in construction, either to build upon, or as construction material. Unlike the more familiar transported sediment soil, the engineering properties and behaviour of tropical residual soils may vary widely from place to place depending upon the rock of origin and the local climate during their formation; and hence are more difficult to predict and model mathematically. Figure 2.1 summarizes the typical process of soil formation.

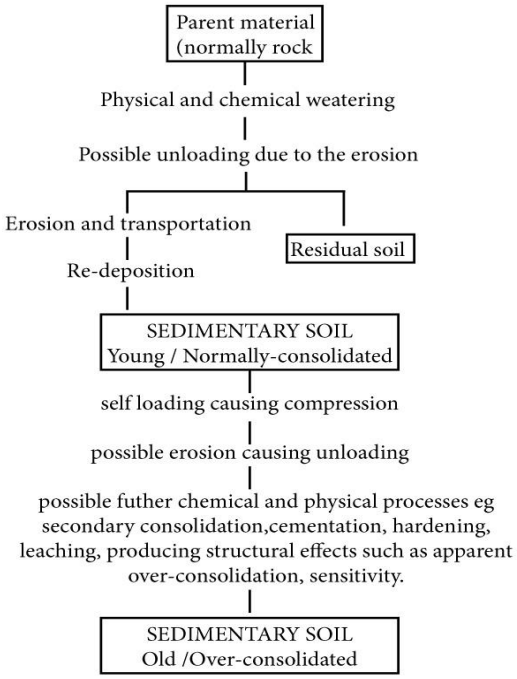

Figure 2.1 – Diagrammatic representation of soil formation processes

The origin and peculiar features of these naturally structured soils requires a more specific approach to the understanding and characterisation of the behaviour beyond those traditionally considered for transported soils. The formation of residual soils occurs by the in-situ weathering of the parent rock, by three major processes: physical, chemical and biological. In the weathering process, the rock and its minerals are gradually broken, releasing internal energy and forming substances with a lower internal energy, hence more stable. Stress release by erosion, differential thermal strains or ice and salt crystallization are examples of physical processes, which degrade the rock, expose its surface to potential chemical attacks and increase its permeability (Blight, 1997). On the other hand, decomposition, leaching, dehydration and oxidation are some of the chemical processes, which tend to alter the rock minerals into clay minerals. Biological processes may include both physical and chemical actions, such as splitting by the intersection with roots or bacteriological oxidation.

Physical weathering is more predominant in dry and moderate climates, while chemical weathering processes are directly related with the humidity and temperature, thus more evident in sub-tropical and tropical zones. Therefore, certain types of rock, which can be greatly affected by the chemical decomposition in tropical regions, produces soils with distinct characteristics of the soil produced by the same type of rock, but more temperate climatic conditions.

2.1.2. TYPICAL PROFILE OF RESIDUAL SOIL

In the North-Western Region of Portugal residual soils from granite are dominant (Viana da Fonseca et al., 1994). The process of formation of a residual soil profile is obviously extremely complex, difficult to understand and difficult to generalize.

It is evident that apart from a few valid generalizations, it is hard to relate the properties of a residual soil directly to its parent rock. Each situation requires individual consideration and it is rarely possible to extrapolate from experience in one area to predict conditions in another, even if the underlying hard rock geology in the two areas is similar (Blight, 1997). The chemical changes and sequences of mineral formed during the weathering are extremely complex.

Weathering processes take place in a large scale (Viana da Fonseca, 1996). Coarse and resistant quartz grains are bonded by fragile clayey plagioclase bridges and result in soils with medium to high porosity fabric. The feldspars are subjected to intense weathering processes, typical of high average annual precipitation and well-draining ground profiles.

The most intensely weathered zones are the classes of W5 and W6 (ISSRM, 1981, IAEG, 1981) that may be described as follows:

- W5: the rock is completely weathered – decomposed and/or disintegrated to soil. The original mass structure is still largely intact. These soils are usually designated as “saprolitic soils” or “young residual soils”;
- W6: all rock is converted to soil. The original mass structure and material fabric have been destroyed. There may be a significant change in volume, but the soil has not been transported. These soils are associated with granular matrices with no leaching and structuration and in tropical regions turn into “lateritic soils” or “mature residual soils”, by secondary processes of re-cementation.

The degree of weathering and extent to which the original structure of the rock mass is destroyed, generally varies with depth from the ground surface. This led to the definition of a typical residual soil profile consisting of three indistinctly divided zones (Vargas and Pichler, 1957; Ruxton and Berry, 1957; Little, 1969; Blight, 1997), depicted in Figure 2.2. The upper zone usually consists of highly weathered, eventually leached soil; the intermediate zone also consists of highly weathered material, though some features of the structure of the parent rock remain, including occasional intact blocks.

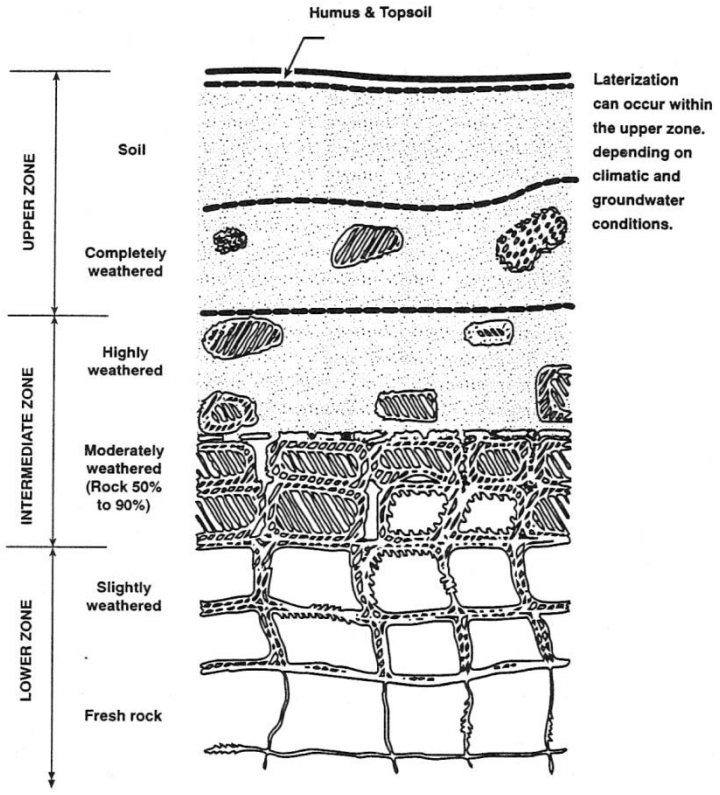

Figure 2.2 - Schematic diagram of a typical residual soil profile (after Little, 1969)

Most of the ground masses that involve geotechnical works in the Porto region, and concern geotechnical designers, are included in the W5 group (Viana da Fonseca, 2003). As pointed out by

(Viana da Fonseca, 1996), depth of weathering ranges typically from 0 to 20 m with more common values of 5 to 9 m.

2.1.3. PHYSICAL PARAMETERS OF RESIDUAL SOIL

Residual soil from granite has a set of widely varying physical properties that depend on the degree of weathering. In these saprolitic soils, those physical parameters usually take the following values for dry apparent densities ($d = \gamma_D / \gamma_W$):

- Sound granites (W1): 2.55 - 2.70;
- Medium to compact weathered altered granites (W2 - W4): 2.30 - 2.60;
- Saprolitic soils (decomposed granites, W5): 1.45 - 1.77.

Is also important to note that the distinction between the intermediate weathering degrees is made by means of other specific indices, namely those of Rock Mechanics classifications for geotechnical design, such as RMR (Bieniawski, 1976) or Q (Barton et al., 1974). These different weathering degrees can be classified according to the uniaxial compressive strengths and characteristics of joints, defining each geomechanical unit (ranging from W1 to W5), as presented in Table 2.1.

Table 2.1 - Typical values of uniaxial compression strength for different weathering classes (Viana da Fonseca, 2003)

Weathering degree	**W_2-W_3 W_3-W_2**	**W_3**	**W_3-W_4 W_4-W_3**	**W_3**	**W_3-W_4**	**W_3**
σ_U (MPa)	≈ 10	≈ 35	≈ 20	≈ 15	≈ 10	0.03-0.14

Typical values of the most common physical parameters for saprolitic residual soils from Porto are presented in Table 2.2. The relatively low values of total unit weight, typically between 17 and 19 kN/m³, are associated with a flocculated structure, with open continuous voids in a cemented, bonded structure (Viana da Fonseca, 2003).

Table 2.2 - Common natural physical parameters (Viana da Fonseca, 2003)

γ_s (kN/m^3)	**w** (%)	**γ_d** (kN/m^3)	**S_r** (%)	**e**	**k** (m/s)
25.7 - 26.5	15 - 25	15.0 - 18.5	80 - 100	0.40 - 0.70	10^{-6} – 10^{-5}

Another relevant aspect is related to the grain size distribuition of this type of soil , that can provide a indication of the degree of weathering of the material. Viana da Fonseca et al. (1994), studied the envelope of more than one hundred grainsize distribution curves obtained in previous works on residual soil from Porto granite. Figure 2.3 shows the size distribution curves that were the result of this work.

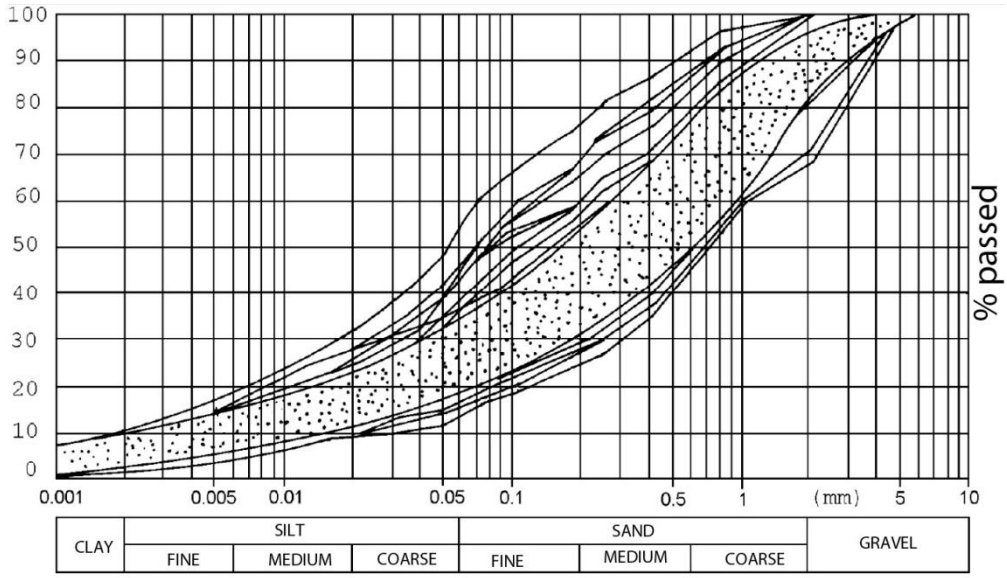

Figure 2.3 - Grain-size distribution curve of residual soil from Porto granite, Viana da Fonseca et al. (1994)

As we can observe from the previous curves, residual soils have a very well graded grain size, with the presence of all type of granulometry. The fine fraction is about 30%, while the sand fraction is predominant with values that may raise 60% of the total weight. The gravel fraction is always present and represents about 20% of the total material weight.

2.2. ELASTIC PROPERTIES OF SOIL

2.2.1. INTRODUCTION

The stress-strain modulus, shear modulus and Poisson's ratio are the principal elastic properties of interest. Both the stress-strain modulus E_S and Poisson's ratio μ are of use in evaluating foundation settlements. They may also be used to back-compute the modulus of subgrade reaction K_S. The shear modulus G is use in soil dynamics problem to compute amplitudes of vibration.

Several modules can be defined to describe soil stiffness as shown in Figure 2.4. Monotonic loading enables to define, at a point such as P a secant modulus G_S and a tangent modulus G_t. In case of cyclic

loading, these modules are relevant only to the loading part of the first cycle. For the subsequent cycles, the defined shear modulus is implicitly the equivalent shear modulus G_{eq}.

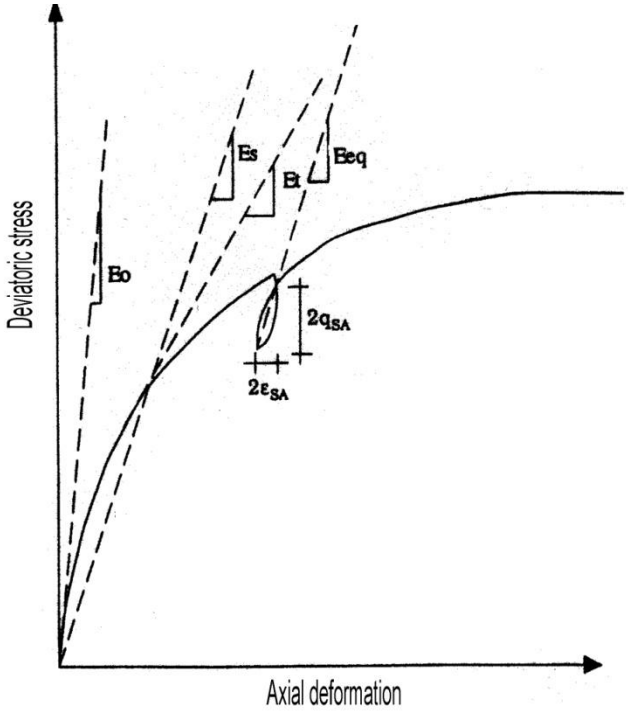

$$E_0 = \lim_{\varepsilon_a \to 0} \frac{dq_0}{d\varepsilon_a}$$

$$E_t = \frac{dq_0}{d\varepsilon_a}$$

$$E_s = \frac{q - q_0}{\varepsilon_a}$$

$$E_{eq} = \frac{q_{sa}}{\varepsilon_{sa}}$$

Figure 2.4 - Definition of soil stiffness

Poisson's ratio μ is defined as the ratio of lateral strain ε_S to longitudinal strain ε_1 when the applied stress is uniaxial (Figure 2.5a) or:

$$\mu = \frac{\varepsilon_3}{\varepsilon_1} \tag{2.1}$$

The modulus of subgrade reaction is defined as the ratio of stress to deformation as shown on Figure 2.5b. The unit of K_S are the same as unit weight.

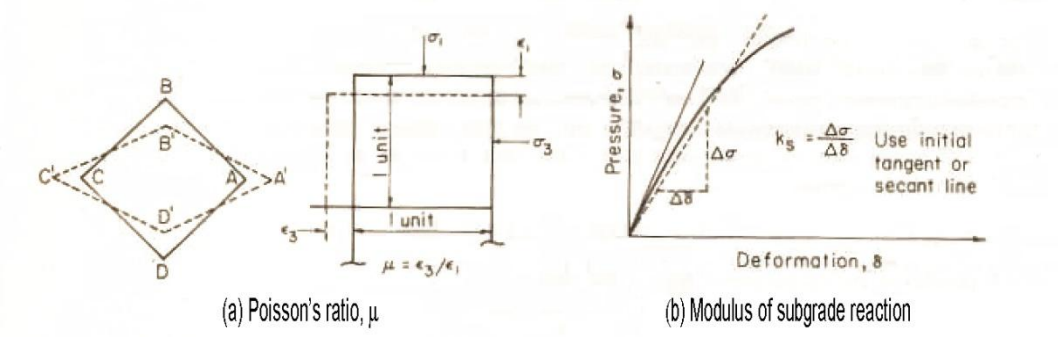

Figure 2.5 - Elastic properties of soil

The shear modul G is defined as the ratio of shear stess to shear strain. It is related to E_S and μ as:

$$G = \frac{s}{\varepsilon_S} = \frac{E_S}{2(1+\mu)} \tag{2.2}$$

The shearing strain ε_S is the change in right angle at any corner of an element as Figure 2.5a such that:

$$\varepsilon_S = angleBCD - angleB'C'D' \tag{2.3}$$

Another concept occasionally used is the volumtric strain, defined as:

$$\varepsilon_V = \frac{\Delta V}{V} \tag{2.4}$$

The bulk modulus E_b is definited as the ratio of hydrostatic stress to the volumetric strain ε_V:

$$E_b = \frac{2}{3} G \frac{1+\mu}{1-2\mu} = \frac{E_S}{3(1-2\mu)} \tag{2.5}$$

Since G and E_b cannot be negative, Eqs. (2.2 and 2.5) set the limit of μ as:

$$-1 \le \mu \le 0.5 \tag{2.6}$$

It appears that the range of μ for soil is 0 to 0.5. Satured soil have $\mu \to 0.5$ and dry soil have $\mu \to 0.5$.

Hooke's generalized stress strain law in terms of principal strains e and stresses s can be written in mattrix notation as:

$$\varepsilon_V = D\sigma \tag{2.7}$$

Where the mattrix D contains Poisson's ratio as:

$$D = \begin{pmatrix} \epsilon/\sigma & 1 & 2 & 3 \\ 1 & 1 & -\mu & -\mu \\ 2 & -\mu & 1 & -\mu \\ 3 & -\mu & -\mu & 1 \end{pmatrix} \tag{2.8}$$

For the CD or CU triaxial test with a cell pressure $\sigma_3$and the deviator stress $\Delta_{\sigma 1}$ acting, we have:

$$\varepsilon_1 = \frac{1}{E_s}(\Delta\sigma_1 - 2\mu\sigma_3) \tag{2.9}$$

If we plot the stress strain data and draw a smooth curve through the point, we shoul be able to solve Eq. (2.9) for E_S and μ by taking $\Delta_{\sigma 1}$ and ε_1 at closely spaced intervals so a linear variation can be assumed in the tangent modulus E_S. The result is the tangent modulus and μ for that stress level. If this

is done on a large number of closely spaced points and the initial value of ε_1 is very close to 0.0, we find the Poisson's ratio exceeds 0.5 at very small strain values. This can be interpreted that most of the stress-strain curve is in the plastic range of strain. This type of analysis also verifies that both E_S and μ are stress-dependent.

Equation (2.9) indicates that the unconfined ($\sigma_3 = 0$) compression test will produce larger axial strain ε_1 at the same stress level compared with triaxial values. This is why the unconfined compression test produces smaller values of E_S often too small by a factor af 4 or 5.

The initial tangent modulus is most often use for E_S. This is for several reason:

- Soil is elastic only near the origin;
- There is less divergence between all plots in this rerion;
- The largest values are obtained often three to five times larger than a tangent or secant modulus from another point along the curve.

In spite of these severlal shortcomings for E_S the value along the curve is commonly used in finite-element analyses based on the computed stress level. This may require that the problem be iterated several times until the computed stress level that was usedon the previous cycle to obtain E_S.

A number of investigator (Leonards, 1968; Sodermanet al., 1968; Makhlouf and Stewart, 1965; Larew and Leonards, 1962) have proposed that a better initial tangent modulus is obtained by cycling the deviator stress tosome stress level about five times and then falling the sample. The initial tangent modulus by this method is somewhat higher than on the first cycle. The method just described is to obtain a static (or resilent) stress-strain modulus value. Cyclic test where the cycles are in terms of low-amplitude strains and frequencies in the range of 1/6 to 10 Hz are used to obtain dynamic values of E_S and G. The dynamic stress-strain modulus may be two to ten times the static value.

Both the stress-strain modulus and Poisson's ratio areheavily dependent on:

- Method on performing the compression test (unconfined, confined, compression, extension, U, CU or CD);
- Confining cell pressure σ_3. E_S tends to increase nonlinearly with an increase in confining pressure;
- Overconsolidation ratio OCR;
- Soil density. E_S increases with particle packing;
- Water content of soil. Lower water contents tend to higher values. Brittle fractures at low strains occur at low water contents;
- Strain rate. At low strain rates the modulus value can be lower by a factor of 2 or more compared with the value obtained at a high test rate (Richardson and Whitman, 1963);

- Sample disturbance.

The stress-strain curve for all soils is nonlinear for all except a possible short segment near the origin. Konder (1963) proposed that the stress-strain curve could be reppresented by a hyperbolic equation of the form:

$$\sigma_1 - \sigma_3 = \frac{\varepsilon}{a + b\varepsilon} \tag{2.10}$$

which could be rewritten with $\Delta_{\sigma 1} = \sigma_1 - \sigma_3$ in linear form as:

$$\frac{\varepsilon}{\Delta\sigma_1} = a + b\varepsilon \tag{2.11}$$

The left side of Eq. (2.10) can be computed for various values of deviator stress and the corresponding strain to make a linear plot. Extension of the plot across the discontinuity at $\varepsilon \to 0$ gives the coefficient a, and the slope is b. While Kondner proposed this procedure for clay soils, it should be applicable for all soils with similar stress-strain curves (see Duncan and Chang, 1970).

Several significant and common methods for stiffness measurement in situ and in the laboratory will be presented in the next paragraph. The information in the following sections was compiled from reference works in the literature, namely from Lo Presti (1995), Stokoe and Santamarina (2000), Lo Presti et al. (2001), Santamarina et al. (2001), Muir Wood (2004), among others.

2.2.2. STIFFNESS MEASUREMENT IN SITU

2.2.2.1. Geophysical methods

A geotechnical geophysical survey is often the most cost-effective and rapid means of obtaining subsurface information, especially over large study areas (Sirles, 2006). Geotechnical geophysics can be used to select borehole locations and can provide reliable information about the nature and variability of the subsurface between existing boreholes. An isolated geologic structure such as a limestone pinnacle might not be detected by a routine drilling program. An effective geophysical survey however, could detect the presence of the pinnacle and map the height and aerial extent of the same.

Other advantages of geotechnical geophysics are related to site accessibility, portability, noninvasiveness, and operator safety. Geophysical equipment can often be deployed beneath bridges and power lines, in heavily forested areas, at contaminated sites, in urban areas, on steeply dipping slopes, in marshy terrain, on pavement or rock, and in other areas that might not be easily accessible to

drill rigs or cone penetration test (CPT) rigs. Also, most surface-based or airborne geophysical tools are noninvasive and, unlike boring or trenching, leave little if any imprint on the environment.

The use of geophysical methods does not preclude the use of intrusive methods on the same site. There can be no substitute for the information obtained from boreholes and trial pits. Geophysics, providing undisturbed in-situ measurements, can be used to its best advantage as an integral part of an investigation which includes intrusive methods.

McCann et.al. (1997) stress that geophysical survey data on its own only measures the vertical and lateral variation of the physical properties of the materials below ground, and that this information can only be interpreted in the light of some knowledge of the likely ground conditions/geology.

This Table 2.3 presents brief summaries of 10 geophysical methods that are commonly employed for geotechnical purposes.

Table 2.3 - General applicability of selected non-invasive geophysical methods to typical site assessments and monitoring objectives

GEOPHYSICAL METHOD	MEASURED PARAMETERS	PHYSICAL PROPERTIES
Shallow Seismic Refraction	Travel times of refracted seismic energy (p- or s- wave).	Acoustic velocity (function of elastic moduli and density).
Shallow Seismic Reflection	Travel times and amplitudes of reflected seismic energy (p-or s-wave).	Density and acoustic velocity (acoustic velocity is a function of elastic moduli and density)
Seismic Tomography	Travel times and amplitudes of seismic energy (p- or s- wave).	Density and acoustic velocity (acoustic velocity is a function of elastic moduli and density).
Ground-Penetrating Radar(GPR	Travel times and amplitudes of reflected pulsed electromagnetic energy.	Dielectric constant,magnetic permeability, conductivity and EM velocity.
Electro-magnetics (EM)	Response to natural/induced electromagnetic energy.	Electrical conductivity and inductance.
Electrical Resistivity	Potential differences in response to induced current	Electrical resistivity.
Induced Polarization(IP)	Polarization voltages or frequency dependent ground resistance.	Electrical capacitance.
Self Potential(SP)	Natural electrical potential differences.	Natural electric potentials.
Magnetics	Spatial variations in the strength of the geomagnetic field.	Magnetic susceptibility and remanent magnetization.
Gravity	Spatial variations in the strength of gravitational field of the earth.	Bulk density.

2.2.2.2. Other field methods

There are also a number of field testing methods that provide measurements of the stiffness of the soil. According to Schnaid et al. (2004), these field techniques can be broadly divided into :

- non-destructive or semi-destructive tests that are carried out with minimal overall disturbance of soil structure and little modification of the initial mean effective stress during the installation process;
- destructive tests were inherent disturbance is imparted by the penetration or installation of the probe into the ground. Examples of non-destructive methods comprise the self-boring pressuremeter (SBPT) and plate loading tests (PLT), where a set of tools is generally suitable for rigorous interpretation of test data under a number of simplified assumptions. On the other hand, examples of invasive-destructive techniques include cone (CP) and Menard's pressuremeters (PMT) and the Marchetti's flat plate dilatometer (DMT). The self boring pressuremeter (SBPT) is the most sophisticated, useful and informative technique, as it is capable of in situ determination of a number of fundamental parameters, namely the in situ at rest state and the stiffness modulus (Wroth, 1982; Campanella, 1994; Robertson et al., 1994; Fahey, 1998, 2001; Gomes Correia et al. 2004; Fahey et al. 2003, 2007).

2.2.3. STIFFNESS MEASUREMENT IN THE LABORATORY

Laboratory testing plays a vital role in determining the stiffness of soil, but can suffer from various disadvantages:

- It must be possible to sample and prepare specimens of a representative volume of soil. This will not be feasible if, for example, the stiffness of the ground is controlled by widely spaced discontinuities, or if it contains very coarse material, such as cobbles and boulders;
- The specimens must, as far as practical, be undisturbed. Even the most 'undisturbed' samples will have undergone some change in both deviatoric and mean effective stress, which need to be compensated for in some way;
- Advanced laboratory testing may take many weeks or months, and requires sophisticated apparatus used by technical staff trained and experienced in its use.

While much advanced testing is carried out under quasistatic loading, the potential use of laboratory dynamic testing, has also been recognised for some time.

Measurements of stiffness in the laboratory are usually grouped, according to the type of tests from which it is inferred, in dynamic and static tests. According to Dobry and Vucetic (1987) and Tatsuoka and Shibuya (1992), the term 'dynamic tests' indicates tests involving fast (monotonic or cyclic) loading conditions (Lo Presti, 1995). These are generally divided into: seismic tests (using piezoelectric transducers) and resonant-column tests. One of the advantages of seismic wave-based tests is that the same test in the field can be also performed in the laboratory. On the other hand, static

monotonic loading tests include: standard triaxial tests, torsional shear tests, and true triaxial tests, whereby the three principal stresses can be independently controlled.

2.3. BASIC PROPERTIES OF SEISMIC WAVES

2.3.1. INTRODUCTION

Seismic measurements have played a particular role in geotechnical engineering for more than 50 years. The effect of a sharply applied, localised disturbance in a physical medium rapidly spreads over in space, this is commonly addressed as wave propagation (Graff 1975). Analogously a wave is defined as a disturbance that travels in the medium and carries energy (Doyle 1995). Many techniques for soil characterization at very small strain levels are based on measurements of particle motions associated to wave propagation. This is made possible by the strong link existing between wave propagation characteristics and the mechanical parameters of the body, which is interested by the phenomenon.

2.3.2. TYPES OF SEISMIC WAVES

Different modes of propagation can be identified by observing the particle motion relative to the propagation direction. For stress waves propagating far from any boundaries in a uniform medium, two fundamental modes of propagation exist:

- compression waves, also called P-waves, are the longitudinal waves that cause particle displacement in the same direction that the waves propagate. This causes compression when the particle velocity is in the same direction as the wave propagation velocity, and in tension when the particle velocity is in the direction opposite to wave velocity;
- shear waves, also called S-waves, are the waves that generate particle displacements perpendicular to the direction of wave propagation. Shear waves also can be divided into vertical shear (S_V) and horizontal shear (S_H) waves indicating the displacement director.

The above waves are often called body waves, because they travel in the interior of a medium. Figure 2.6 shows the particle motions of planar body waves where the initial condition, the motion of P-waves, and the motion of S-waves are represented in Figure 2.6 a, b, and c, respectively.

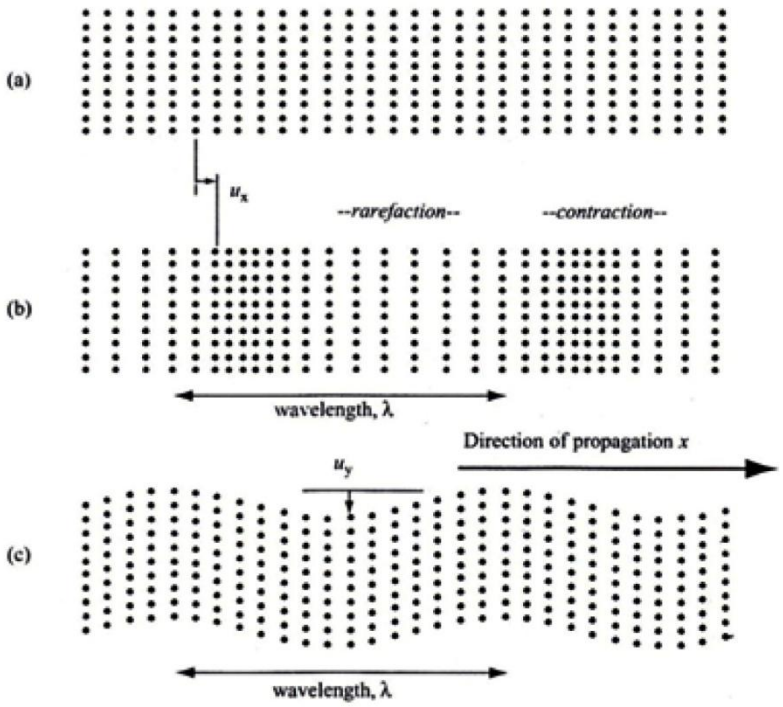

Figure 2.6 - P-wave and S-wave particle motion from Santamarina (2001)

In contrast there are the so-called surface waves, that travel in a very shallow zone close to the free surface of an halfspace. They are essentially of two different kinds:

- Stoneley waves, also known as generalised Rayleigh waves These waves travel across a mechanical impedance (i.e. rV) discontinuity and they rapidly attenuate going away from the interface. It can be shown that such waves can exist only for given values of the ratio between stiffness properties of the two adjacent layers (Graf 1975);
- Love waves, these are basically horizontal shear waves that propagate along the surface.

The latter ones can exist only in presence of a waveguide, i.e. of a softer superficial layer above stiffer materials, and can be seen as generated by multiple reflections of energy trapped in this layer. Their existence was shown by Love in 1911 and the particle motion associated to them is transversal with respect to the direction of propagation. A representation of the particle motion associated to the propagation of surface waves is reported in Figure 2.7.

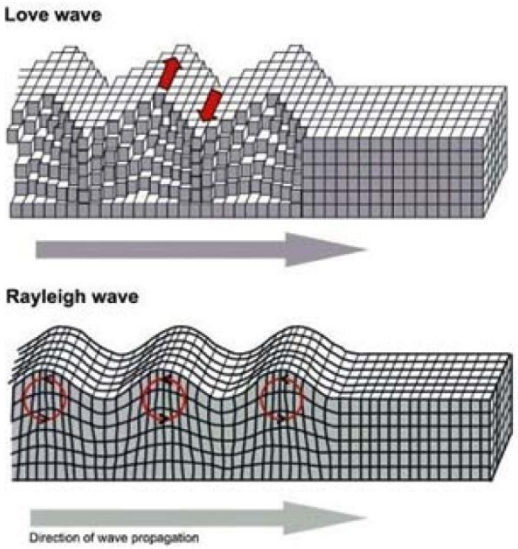

Figure 2.7 - Wave propagation and particle motion of surface waves from Virdi and Rashkoff (2011)

2.3.3. WAVE VELOCITIES

During the last decades shear wave velocity measurements on land were mainly obtained from cross-hole testing with a view of deriving dynamic soil properties required in earthquake engineering. More recently the seismic cone (SCPT) has allowed performing measurement without the need to drill two or three parallel boreholes.

The shear wave velocity V_S is increasingly recognised as a significant parameter for geotechnical engineering. V_S is directly related to the structure of the soil skeleton and is independent of both the water content and the gas content. V_S can be directly related to the small strain shear modulus G_0 of the material which is a key parameter in soil structure interaction problems. The compressive velocity V_P is used to characterise the upper (typically < 5m) seabed sediments.

Stress waves are non-dispersive in a uniform elastic medium. The term non-dispersive indicates that the propagation velocity is independent of frequency. These waves are also considered non-dispersive in lowloss homogeneous soils at small-strains and low frequencies (Stokoe and Santamarina, 2000). However, stratigraphy and other forms of heterogeneity cause frequency-dependent velocity. The "far-field" velocities of elastic stress waves depend on the stiffness and mass density of the material as:

P-wave velocity
$$V_P = \sqrt{\left(\frac{E}{\rho}\frac{(1-\nu)}{(1+\nu)(1-2\nu)}\right)} = \sqrt{\frac{M}{\rho}} \qquad (2.12)$$

S-wave velocity
$$V_S = \sqrt{\left(\frac{E}{2\rho}\frac{1}{(1+\nu)}\right)} = \sqrt{\frac{G}{\rho}} \qquad (2.13)$$

where

- ρ is the mass density;
- M is the constrained;
- G is the shear modulus;
- E is the Young's modulus;
- υ is Poisson's ratio.

For a homogeneous, isotropic material, compression and shear wave velocities are related through Poisson's ratio, υ, as:

$$V_P = V_S \sqrt{\frac{1-\nu}{0.5-\nu}} \tag{2.14}$$

A good approximation for the velocity V_R in terms of V_s and Poisson's ratio is (modified from Achenbach,1975):

R-wave velocity

$$V_R = \sqrt{\frac{0.874 + 1.117\,\nu}{1+\nu}} V_S \tag{2.15}$$

These equations permit computing the relative values of V_P, V_S and V_R as a function of Poisson's ratio. At υ= 0, $V_P = \sqrt{2}V_S$ and V_R = 0.874 V_S. At υ= 0.5 (which theoretically represents an incompressible material; hence, an infinitely stiff material), $V_P = \infty$ so that $V_P/V_S = \infty$. At υ= 0.5, $V_R = 0.955V_S$. The ratios of body wave velocities (V_P/V_S) typically determined with small-strain seismic tests on unsaturated soils are around ~1.5, which corresponds to Poisson's ratio ~0.10; therefore, the small-strain Poisson's ratio is relatively low.

2.3.4 MEASUREMENT OF ELASTIC WAVES IN A LABORATORY

The measurement of soil properties is an intrinsic component in the study of soil mechanics and its application to geotechnical design. Recent research has brought about the development of dynamic methods for the measurement and assessment of soil properties using shear wave velocities generated by piezo-ceramic plate transducers.

A piezoelectric transducer is a device that transforms one type of energy to another by taking advantage of the piezoelectric properties of certain crystals or other materials. When a piezoelectric material is subjected to stress or force, it generates an electrical potential or voltage proportional to the magnitude of the force. This makes this type of transducer ideal as a converter of mechanical energy or force into electric potential. The piezoelectric effect also works in reverse, in that a voltage applied to a piezoelectric material will cause that material to bend, stretch, or otherwise deform.

Originally thought to be a property only of specific types of crystals like quartz and topaz, advances in materials science have resulted in the creation of polymers and ceramics that also show piezoelectric properties. In fact, the most common piezoelectric material currently in use is the man-made ceramic lead zirconate titanate, known as PZT.

Shear-plates and bender elements are examples of piezoelectric transducers, which can transmit and receive S-waves; similarly, extender elements and compressiontransducers can transmit and receive P-waves (Ferreira, 2008). All these piezoelectric transducers can be installed in a wide variety of soil testing devices, from conventional to non-conventional, from static to dynamic equipments. The triaxial cell is probably the most common apparatus where these transducers are used, but its use in other devices have also been reported, namely in the oedometer (Fam and Santamarina, 1995; Zeng and Grolewski, 2005) and direct shear apparatus (Dyvik and Olsen, 1989).

2.3.4.1. Plate transducers

As the name suggests, plate type transducers are flat shaped Piezo-electric transducers consisting of a central core of polarized piezoelectric ceramic sandwiched between two thin electrodes at the top and bottom surfaces (Sarju Mulmi, 2008). There are two types of plate transducers P type (PT-P) and S type (PT-S) generating P and S waves respectively. The nature of the plate transducer i.e. P or S depends upon the direction of polarization. If the ceramic is polarized in the direction parallel to the electrodes then it generates S waves upon the application of voltage. On the other hand, if the ceramic is polarized in the direction perpendicular to the electrode i.e. in the thickness direction then it generates P waves upon the application of voltage. The thickness and the size of the plate transducer can be chosen as per the necessity of the experiment. Example of P and S type plate transducers are shown in Figure 2.8.

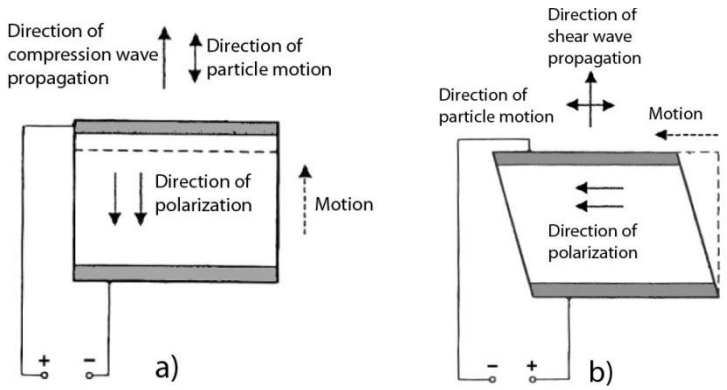

Figure 2.8 - a) Schematic figure of P type plate transducers; b) Schematic figure of P type plate transducers

The difference between the plate transducer and the bender element is twofold: the first is the fact that plate transducers are non invasive compared to bender element because of their flat shape contrary to

the beam like shape of bender element which protrudes into the specimen. Only a thin coupling plate is attached to the top surface of the S type plate transducer to allow sufficient friction between the plate and the soil. The second is the deformation obtained for a given voltage; for the same voltage bender element produces larger deformation than plate transducers hence, plate transducers need larger amplification.

Lawrence (1963, 1965) was one of the first to employ shear type piezoelectric plate transducers in shear wave testing of soil specimens. But after that, plate transducers have received very little attention due to the aforementioned reasons. The setting of plate transducers is similar to that of bender elements.

2.3.4.2. Bender and bender-extender element

The bender-element technique represents the most widely used method for determining V_S in the laboratory (Viana da Fonseca and Ferreira, 2009) and one of the ways of measuring the stiffness at the very beginning of this non-linearity. The use of bender elements in geotechnics began in the late 1970s with Shirley and Hampton and later with Dyvik and Madshus, who showed very good agreement between the results obtained by the bender elements and with resonant-column tests.

A bender element is a piezoceramic element made of two transversely poled plates that are bonded together, as indicated in Figure 2.9. When one end of the element is fixed the excitation of the external voltage will make the opposite end move and the element will bend in the direction normal to the face of the plates. In ideal conditions the transmitter element, embedded in the soil sample, introduces a shear wave into it. Upon the arrival of the shear wave at the other end of the soil sample the receiver element will move and generate a small voltage, which is detected at the electrode and shown on an oscilloscope. The technique is based on a measurement of the arrival time of the shear wave, assuming a plane-wave propagation, i.e., the time difference between the excitation of the transmitter and the excitation of the receiver element.

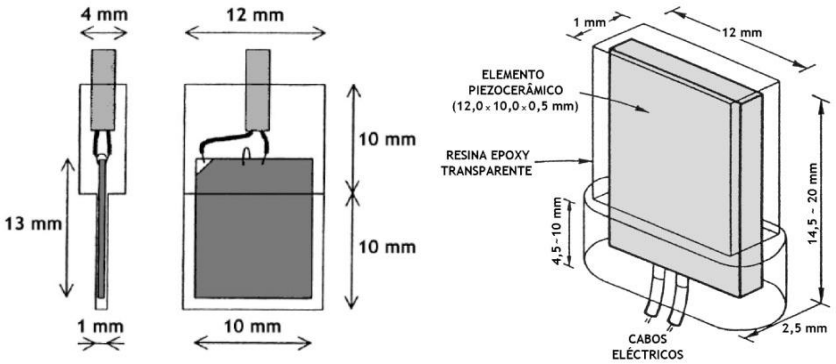

Figure 2.9 - Schematic figure of Bender Element (Ferreira, 2003)

The model presented in Figure 2.9, is still the basis of current design, though variations have been made, namely to its size and to arrangements (usually T-shaped) of pairs of transducers in a single probe (Ferreira, 2008). These variations are consequences of the need to adjust to new testing challenges: in order to observe vertical and horizontal homogeneity in triaxial specimens, and thus assess anisotropy, the standard-sized BE is not appropriate, as it is too large in relation to the travel distance and too heavy to be sustained by the sample. The combination of two bender placed orthogonally in a single probe has also resulted from the interest in measuring vertically- and horizontally-polarized waves. And so, the miniature and/or T-shaped BE have been developed and manufactured with great success, especially when horizontally mounted in a triaxial specimen (Pennington et al., 1997, 2001).

Compression-wave piezoceramic elements (extender elements), on the other hand, are less commonly used as compression wave velocity is less frequently measured. Bender/extender elements [B/EE] were "accidentally" discovered when the typical BE connection scheme was incorrectly performed (Fuertes, 1999). The most interesting feature of this transducer is its reversibility of functions: a parallel-connected bender-extender element works as an S-wave transmitter [BT] and a P-wave receiver [ER]; on the other hand, a seriesconnected B/EE is both a P-wave transmitter [ET] and an S-wave receiver [BR]. Figure 2.10 and Figure 2.11 detail its configuration and wiring for S- and P-wave measurement, respectively.

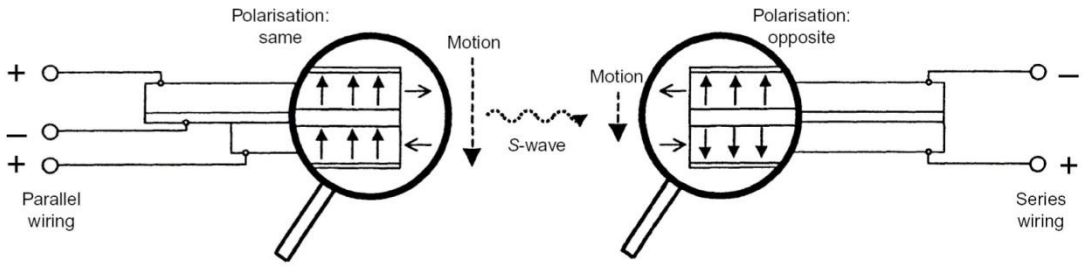

Figure 2.10 - Typical BE wiring details and operation: a) transmitter; b) receiver (after Lings and Greening, 2001)

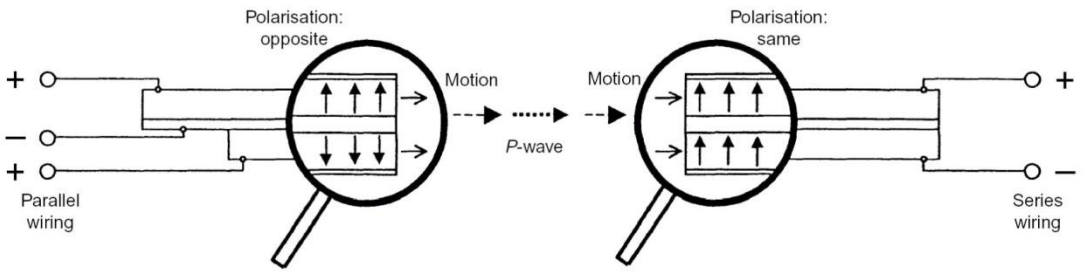

Figure 2.11 - Typical EE wiring details and operation: a) transmitter; b) receiver (after Lings and Greening, 2001)

2.3.5. THE SENSITIVITY OF S WAVE TO SEVERAL FACTORS

The shear wave velocities, and therefore also the maximum dynamic shear modulus, are highly sensitive to a number of relevant factors and soil conditions. In contrast, since compression waves travel through both solids and fluids, the response in saturated conditions is dominated by the presence of water and does not characterise the behaviour of the saturated soil correctly.

Hardin and Black (1969) were the first to systematise the more relevant factors influencing the overall shear modulus, in a generic function such as:

$$G_0 = f(\sigma', e, H, S, \tau_{oct}, C, f, t, \zeta, T) \quad (2.16)$$

where σ' represents the effective stresses, e is the void ratio, H is the stress history, S is the degree of saturation, τ_{oct} is the octahedral shear stress, C refers to grain and mineralogical properties, f is the excitation frequency, t is time (ageing), ζ is a measure of the fabric and structure of the soil, and T is the temperature.

Clearly, the influence of each of these factors in stiffness is varied. It is widely recognised that the most important factors to which the stiffness is dependent of are the principal effective stresses in the wave propagation and wave polarisation directions, the void ratio, the structure or packing of the soil, and also the degree of saturation (mainly for clays and silts), also associated with suction levels, and the degree of cementation (natural or artificial).

Hardin and Blandford (1989) presented a formulation incorporating the fundamental and most influential parameters, as follows:

$$G_{0ij} = S_{ij} \cdot F(e) \cdot OCR^{\,k} \cdot p_a^{(1-n_i-n_j)} \cdot (\sigma'_i)^{n_i} \cdot (\sigma'_j)^{n_j} \quad (2.17)$$

where σ'_i and σ'_j principal effective stresses in the wave propagation direction, i, and wave polarisation direction, j; k is an empirical exponent of the overconsolidation ratio OCR depending on the plasticity index, IP; f(e) is a void ratio function, S_{ij} is a non-dimensional material constant reflecting the fabric and structure of the soil; n_i and n_j are empirical stress exponents or indices (for sands, $n_i \approx n_j$ is often assumed), and p_a represents a reference stress, usually the atmospheric pressure (taken equal to 1 kPa).

According to several authors, the influence of the overconsolidation ratio can be neglected if an appropriate void ratio function is considered (Tatsuoka and Shibuya, 1992; Jamiolkowski et al., 1995; Barros, 1997; Sulkorat, 2007). For the definition of the void ratio function, three reference expressions are usually considered, as indicated in Table 2.4. These can be directly applied when no specific study

is carried out to determine which is most suitable for the soil in study, or serve as a starting point for a more soil-specific analysis. The differences between these reference voidratio functions are more evident at low void ratios, as illustrated in Figure 2.12.

Table 2.4 - Reference void ratio functions (from Ferreira, 2003)

Function	General expression	References
F(e)1	$\frac{(2.17 - e)^2}{1 + e}$	Hardin e Richart (1963);Iwasaki et al. (1978)
F(e)1	$\frac{1}{0.3 + 0.7 \cdot e^2}$	Hardin (1978); Chung et al. (1984)
F(e)1	$e^{-x}, x = 1.3$	Lo Presti (1995); Jamiolkowski et al. (1991)

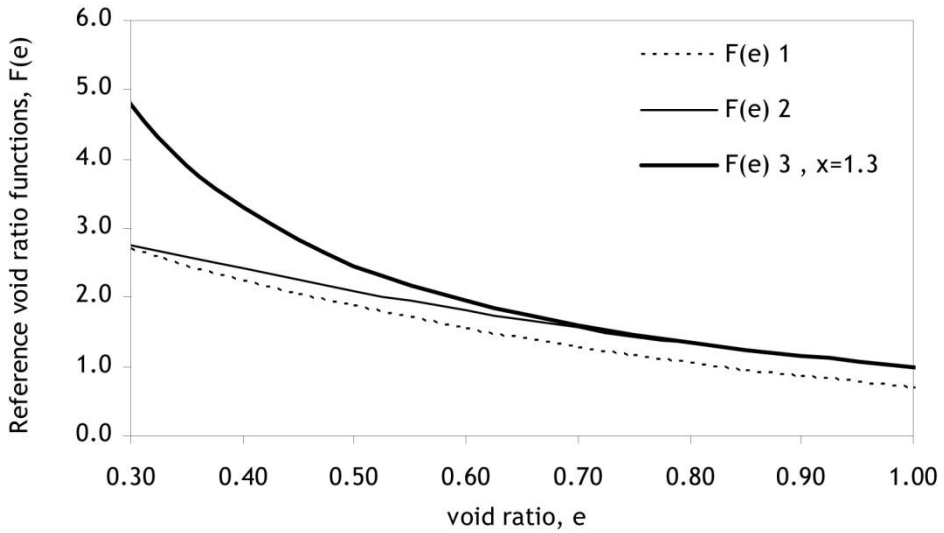

Figure 2.12 - Differences between reference void-ratio functions against void ratio

In standard triaxial testing, the stresses acting in the wave propagation and polarisation directions corresponding to the principal vertical and horizontal stresses. When only the vertically propagated shear waves are measured, the generic form of Equation 2.17 can be simplified to:

$$G_{0vh} = S \cdot F(e) \cdot (\sigma'_v \cdot \sigma'_h)^{n_{vhj}} \tag{2.18}$$

When horizontally propagated shear waves are also measured, the individual indices can be directly extracted. Strictly under K or K_0 stress conditions (where the horizontal and vertical stresses are proportional), the fundamental expression of G_{0ij} can be modified into three separate equations:

$$G_{0hv} = S_{hv} \cdot F(e) \cdot K^{n_h} \cdot \sigma'^{n_{hv}}_v \tag{2.19}$$

with $n_{hv} = n_h + n_v$

$$G_{0hh} = S_{hh} \cdot F(e) \cdot K^{n_{hh}} \cdot \sigma'^{n_{hh}}_{v} \quad (2.20)$$

with $n_{hh} = 2 \cdot n_h$

$$G_{0vh} = S_{vh} \cdot F(e) \cdot K^{n_h} \cdot \sigma'^{n_{vh}}_{v} \quad (2.21)$$

with $n_{vh} = n_v + n_h$

Several authors (e.g. Pennington, 1999) have suggested that the out-of-plane stress has negligible influence on G_{0ij}. Nevertheless, the influence of all stresses involved can be assessed by considering the relationship with p', which may be especially useful towards understanding the response in three-dimensional conditions, which can be expressed as follows:

$$G_{0ij} = S_{ijo} \cdot F(e) \cdot p'^{n} \quad (2.22)$$

This concept behind these formulations will serve as basis for the presentation, analysis and discussion of the results obtained in the laboratory tests carried out in this research. The normalisation of the different shear moduli in relation to the void ratio enables to directly compare the influence of the applied stresses and, simultaneously, identify the structure parameter S. For this purpose, the normalised shear modulus in relation to the void ratio is denoted with an asterisk:

$$G_{0ij}^{*} = \frac{G_{0ij}}{F(e)} \quad (2.23)$$

The consideration of different approaches to the stress-dependency of the shear moduli aimed at defining which is most appropriate, mainly from the interpretation of results in true triaxial conditions.

2.4. ASSESSMENT OF SAMPLING QUALITY

2.4.1. INTRODUCTION

One of the essential elements involved in the geotechnical analysis and design, which is vital to their success, is precise estimation of engineering properties of soils from results of laboratory testing in which the stresses, deformations and boundary conditions of soil specimens can be readily and precisely controlled and observed. In order to obtain highly representative and reliable soil design parameters by means of laboratory tests, the engineering properties of the soil such as the shear strength and compressibility must be determined through appropriate testing of undisturbed samples previously retrieved from the ground using some form of sampling procedure (Joyce, 1982; Clayton et al., 1995).

However, samples obtained from field sampling may suffer from sampling disturbance to certain degrees that generally cause wide discrepancies in properties between soil specimens tested in the

laboratory and the in-situ soils. These disturbances have been regarded as a significant adverse problem to the geotechnical engineers because it always leads to poor acquisition of realistic soil parameters. It follows that the requisite for a successful acquisition of the information of geotechnical parameters is to proper accounting for the analysis and assessment of the disturbance of soils during sampling. In order to secure a formal basis for quantifying complexities and uncertainties involved in sampling disturbances in a systematic and rational manner, it is necessary to study specifically and minimize the amount of disturbance at every stage during sampling in order to obtain high-quality laboratory tests results. In the light of this fact, the disturbance sources should be isolated individually for study.

Santagata & Germaine (2002) stated that while many studies have attempted to assess sampling disturbance under specific conditions, only two models that rationally quantify the effects of sampling disturbance have been proposed. They are the "perfect sampling approach" (ladd e Lamble, 1963; Skempton e Sowa, 1963), and the "ideal sampling approach" (Baligh et al. 1987). The "perfect sampling approach" considers only the disturbance due to the in-situ stress release while the disturbance simulated based on the "ideal sampling approach" has shown that soil elements located inside a sampler tube undergo a complex strain istory involving both shear and normal strains.

Baligh et al. (1987) has provided many important insights into this problem in which strains are developed as a sampler is pushed into the ground and pointed out that the effect of disturbance due to penetration has the largest impact on the sampling disturbance and therefore further improvement on this stage is necessary. Experience suggests that the disturbances associated with the withdrawal of the sampler from the ground, and the subsequent extrusion of the sampler from the sampler tube , will be small in comparison with the effects of displacing the soil around the sampling tube during driving, provided that good practice is adhered to (Clayton et al., 1998).

2.4.2. SAMPLE DISTURBANCE

Perfect sampling represents one of the greatest challenges in geotechnical engineering. A sample of soil obtained by any sampling process will suffer disturbance, which can be divided into two main sources. The first is stress relief and the second is mechanical disturbance. Stress relief refers to the undrained removal of the in situ anisotropic stress state during borehole drilling, and is an unavoidable effect of removing soil from the subsurface. Stress relief additionally occurs when samples are removed from the subsurface sampling stress state to isotropic atmospheric pressure at the surface (i.e., $\sigma_{tot} = 0$). This phenomenon typically causes negative pore water pressures to develop, the amount of which relates to pore size and distribution, and saturation (Gilbert 1992).

Mechanical disturbance refers to shear-induced disturbance that affects soil structure and stress state. It is related to sampling and specimen preparation tools/equipment/techniques and operator performance (Baligh et al. 1987). It occurs as a result of borehole advancement, sample tube penetration, sample recovery, water content and pore water pressure within the sampled soil, extrusion from the tube, drying, and laboratory test specimen preparation (Gilbert 1992, Hvorslev 1949). One of the most significant advances in the last decades in understanding disturbance by tube sampling has been the introduction of the strain path method (Baligh, 1985; Baligh et al., 1987) and its application to the deep penetration of a sampling tube into the ground, thus providing an analytical basis upon which the effects of sampling could be evaluated (Hight, 1993, Hight, 2000).

Geometry and size of the tube are important factors for controlling sample quality, especially the geometry of the cutting shoe (Clayton et al. 1998). Figure 2.13 show the geometry of a soil sampler. Hvorslev (1949) estabilished several parameters that relate tube geometry to the affect it has on the retrived samples, which are expressed in the following equations.

Recovery Ratio: $RR = \frac{L}{H}$ (2.24)

Inside Clearance Ratio: $ICR = \frac{ID - D_i}{D_i}$ (2.25)

Outside Clearance Ratio: $OCR = \frac{D_e - OD}{OD}$ (2.26)

Area Ratio: $AR = \frac{D_e^{\,2} - D_i^{\,2}}{D_i^{\,2}}$ (2.27)

Length to Diameter Ratio $= \frac{L}{D}$ (2.28)

where

- L is the lenght of the recovered sample;
- H is the sampler penetration lenght;
- ID and OD are the inside and outside diameters of the sampling tube;
- D_i and D_e are the inside and outside diameters of the cutting shoe;
- α and β are the outside and inside of the cutting edge angle.

.

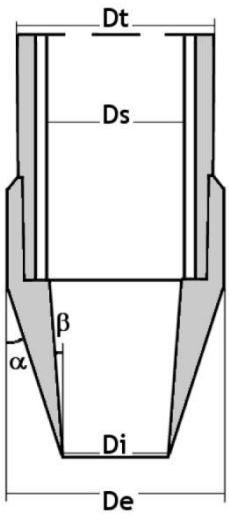

Figure 2.13 - Definition of the geometric parameters of a tube sampler

RR indicates how much soil is retained during the push. When RR < 1, soil may have fallen out of the tube during extraction or soil may have been compressed as a result of sidewall friction. RR > 1 values potentially indicate that basal soils heaved into the borehole prior to sampling or that excess soil at the bottom of the borehole were not removed prior to sampling.

AR represents the amount of soil that is displaced when the sampler is pushed into the subsurface. Hvorslev (1949) reccomends an AR of less than 10%, as larger AR values result in greater resistance of the sampler to penetration and potential for disturbance. Greater projected areas result in more soil displacement , which typically displace into the sampler cavity. Greater area rations may be used when a piston sampler is used to keep excess soil from entering the sampler and the tube edge is sharp with a small cutting angle.

For tubes with inside clearance (ICR > 0), there is a reduction in sidewall friction during sampling, which reduces the amount of disturbance from soil shearing along the soil-tube interface. For "undisturbed" sampling, Hvorslev (1949) recommends an ICR between 0.75 and 1.5% for long tubes and 0.5% for short tubes.

OCR (outside clearance ratio) pertains to samplers with an attachable cutting shoe with an outside diameter greater than that of the tube's outside diameter. This geometry is typically employed to reduce friction between the soil deposit and tube. For cohesive soil, a small value of OCR (2% to 3%) may decrease the resistance of the sampler to penetration, but care should be taken in very soft or cohesionless soils, where the soil can collapse against the outside of the tube re-establish side friction (Hvorslev, 1949).

Extracting the sample inevitably involves removal of the boundary stresses and disturbance is caused by sampling, transportation, and trimming before stresses are reimposed in the laboratory (Hight, 2001; Ladd & DeGroot, 2003). The stress and strain paths experienced by the sample are dependent on the method of sampling. Ladd & Lambe (1963) showed that changes in the residual effective stress inside the sample during the sampling process might cause differences in soil behaviour. Baligh (1985) and Baligh et al. (1987) analytically predicted soil deformation resulting from penetration of a sampling tube using the strain path method. Figure 2.14 illustrates potential sources of sample disturbance via a hypothetical stress path during the process of obtaining a tube sample for laboratory testing.

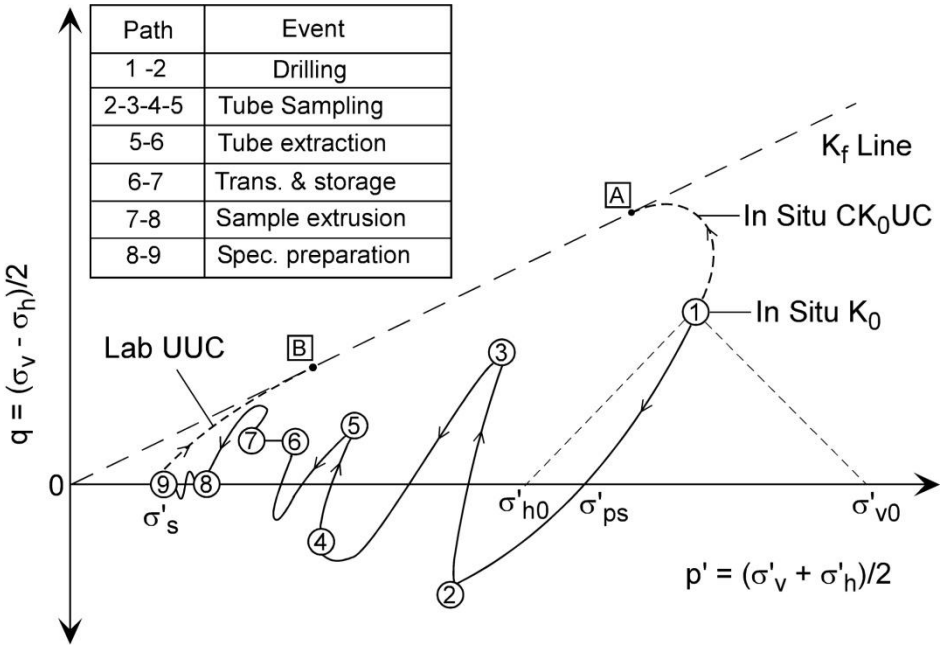

Figure 2.14 - Stress path during tube sampling and specimen preparation of centerline element of low OCR clay (Ladd and Lambe, 1963, Baligh et al., 1987, in Ladd and DeGroot, 2003)

Their results showed that a soil element entering a sample tube is subjected to a complex strain path depending on its location. The element at the centreline of the sample experiences the minimum distortion as it is subjected to undrained compression as the tube advances towards it, followed by undrained extension of the same magnitude once the sample is inside the tube, and followed by recompression to its initial shape when it has penetrated well inside the sample tube. The imposed strain magnitude was found to vary with the ratio between the sample diameter and the thickness of the sample tube and also with the inside clearance ratio. During penetration of a tube sampler, shear distortion occurs near the inside surface of the sample tube and the soil at the perimeter is then remoulded. The consequent difference of suction between the periphery and centre of the sample causes subsequent migration of water within the sample during sample storage, leading to a variation

of the moisture content. Though mainly developed for sampling of soft clays, these studies can be generalised to any sensitive and/or structured.

2.4.3. SAMPLE QUALITY ASSESSMENT PROCEDURE

No definitive method exists to determine the absolute sample quality vis-à-vis the "perfect sample". Okumura (1971) proposed the following requirements for a sample quality assessment procedure, which should be met in order for the method to be consistent and effective. The autor stated that a sample quality parameter must be:

- Easy to determine for undisturbed conditions;
- Consistently variable with disturbance regardless of depth, soil type, and stress system;
- Sensitive to changes resulting from disturbance;
- Easily and accurately measured for all specimens.

Several methods have been developed to assess the quality of soil samples, including visual inspection, radiology, and analysis and interpretation of laboratory test data. These methods are discussed in the following section.

2.4.3.1. Visual inspection

Visual inspection of soil samples is useful for identifying gross changes in soil structure. By assessing the conditions and integrity of the tube itself, one can identify damage that may have occurred during sampling or transport, which can indicate potential sample disturbance. In addition, the presence of rocks or voids, remolded areas of clay soils, changes in color from tube rusting, or distortions in the layering pattern for layered soils observed after extrusion are indications that the soil has undergone sample disturbance.

However, only large distortions are visible, generally in the peripheral zones of the sample (Ferreira, 2008); the relatively small strains, associated with yield and damage to a bonded structure, usually occurring around the centreline of the sample, are hardly detected. In Figure 2.15 two examples are provided, where the disturbance caused by the penetration of the sampling tube is clearly visible.

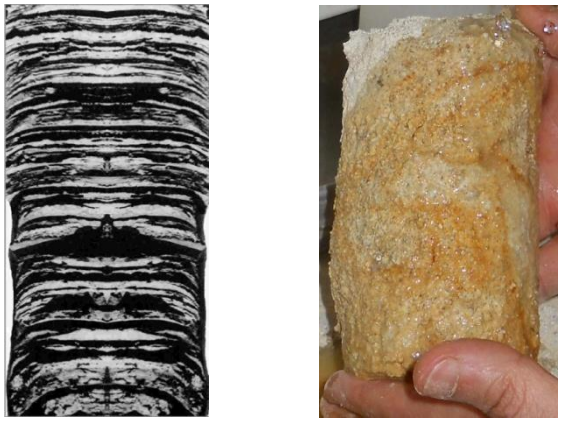

Figure 2.15 - Fabric inspection: a) disturbance on a laminated clay sample with sand and silt layers spaced every 10 mm, Rowe (1972); b) clearly disturbed residual soil sample

2.4.3.2. Radiology

Many geotechnical tests require the utilization of undisturbed representative samples of soil deposits. Many of the samples obtained through undisturbing sampling methods have inherent anomalies that are due to sampling procedures which can cause disturbances of varying types and intensities. These anomalies and disturbances, however, are not always readily detectable by visual inspection of the undisturbed samples before or after testing.

Radiography is mainly performed on undisturbed samples used for highly technical or expensive projects due to the cost and equipment associated with this method. Ladd and DeGroot (2003) recommended that radiology be used on projects where only a few expensive samples have been obtained, which require specialized stress path triaxial testing, in order to identify variations in soil type (to differentiate peat, cohesive, and/or granular soils), macrofabric (layer thickness, inclination, and distortion), intrusions (e.g. rocks and other materials that are inconsistent with the soil body), anomalies (e.g. shear planes, fissures, and fractures), and the variation in the degree of soil disturbance (e.g. bending at the tube surface, stress relief cracks, voids, and gas bubbles).

The basic concept is to place the tube sample in an aluminum holder to create a constant material thickness for penetration and attach a scale with lead letters and numbers to the tube to mark the location that the x-ray photons penetrate the sample tube and soil. Photons are used to penetrate the tube (current and exposure time vary with soil density and tube diameter) and the resulting intensity of these photons as they hit the x-ray film depends on the density and thickness of the soil and tube they pass through.

X-ray radiographs show variations in the ability of x-rays to penetrate matter, these variations are exhibited as varying shades of gray color burned on the X-ray film. Figure 2.16 show some factors that can be discerned from the radiograph.

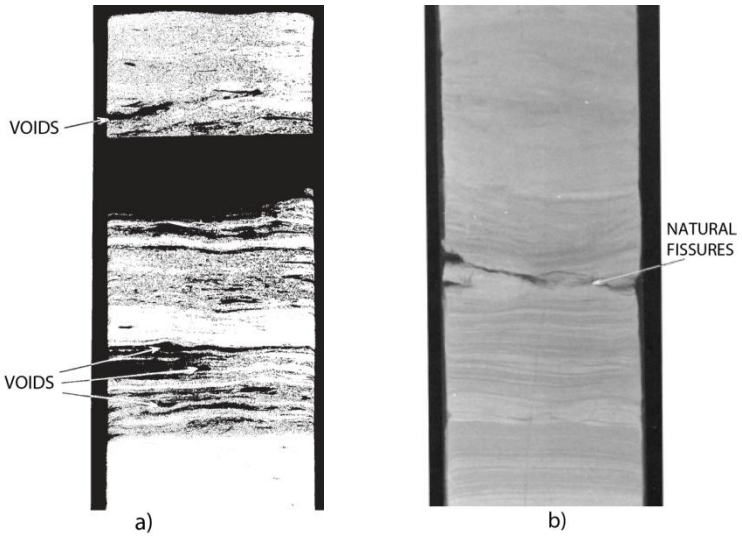

Figura 2.16 – a) Open void spaces will show as dark dots or channels, depending on the shape of the void; b) Where bedding of various layers are apparent in the radiograph, bedding will be continuous across fissures

2.4.3.3. Inspection of laboratory test results

Sample quality can be evaluated by visually inspecting stress-strain and one-dimensional consolidation curves that result from laboratory tests. Lunne et al. (1997) discussed some approaches for the assessment of sample disturbance using laboratory data based on oedometer and triaxial compression tests, that may be described as follows:

- Volumetric strain, ε_{vol}, during reconsolidation to in situ K_0 stress state, where increasing disturbance leads to greater values of ε_{vol};
- Peak shear stress CAUC tests, where better quality samples exhibited greater s_u values;
- Strain at failure from CAUC test. Higher quality samples showed lower failure strains at the peak s_u;
- Preconsolidation stress, σ'_p, constrained modulus, M, and coefficient of consolidation, c_v, from oedometer test result. In general, values of σ'_p, M and c_v are less for lesser quality tube samples than for better block samples, indicating that these parameters decrease with increasing disturbance.
- Small strain shear modulus, G_{max}, from bender element tests. Recent studies have suggested that G_{max} might be useful as a non-destructive test to indicate sample quality, since G_{max} values should decrease with increasing disturbance to the soil structure.

The two most common methods of sample quality assessment for clay soil are based on the measure of volume change during K_0 reconsolidation to the in situ effective stress state. They are the SQD method (Terzaghi et al., 1996), based on e_{vol} at σ'_{v0}, and the NGI method (Lunne et al., 1997), based on normalized change in void ratio, Δ_e/e_0 at σ'_{v0}. Both of these methods assing a number or letter grade

to the specimen indicating the quality, where specimens experiencing little volumetric change are the best quality designated with a A (SQD) or 1 (NGI), and specimens experiencing large strains are given designations of E (SQD) or 4 (NGI) indicating very poor quality. The NGI method has two advantages over the SQD method , which are the use of e_0 to account for the initial state of the soil and the incorporation of OCR into the methodology to account for initial soil stiffness. (Lunne et al 1997) maintain that the NGI method is a therefore a more sensitive indicator of sample disturbance than the SQD method. Typically, Δ_e/e_0 is smaller for higher OCR soils compared with similar quality lightly overconsolidated (OC) specimens. Moreover, Tanaka et al. (2002) concluded that the parameters of the SQD test cannot be universally applied to represent sample quality. As noted by Hight (2000), the absolute value of the strains will depend on the reconsolidation path followed and the soil compressibility.

2.4.3.3.a). Comparation between laboratory and in situ measurements of seismic wave velocities

New demands in soil mechanics research and geotechnical engineering practice require advanced characterization techniques in both laboratory and the field for monitoring processes and assessing various conditions, especially for those assessments involving sample disturbance (Sasitharan et al., 1994) and the quality control of soil improvement.

The potential for assessment of sample quality using small strain shear stiffness parameters V_s and G_{max} has been under investigation for the last decade. Sample quality assessment method using these parameters are comparative methods, requiring both measurements of in situ V_s typically from downhole, crosshole, or seismic cone penetration testing, as well as measurement of V_s from the soil samples in question, usually from bender element test. The sensitivity of the shear waves enables to distinguish different structure or fabric arrangements, as well as stress conditions and void ratio. Thus, the comparison between laboratory and in situ measurements of seismic wave velocities (or maximum shear modulus) has been increasingly accepted as one of the most promising for the assessment of sampling quality, especially in natural structured soils (Viana da Fonseca and Coutinho, 2008).

For the comparisons to be valid, the laboratory samples must be representative and should be restored to their in situ stress state, because of the dependence of V_s on stress state. In order to account for the influence of void ratio, allowances must be made for changes in void ratio during reconsolidation to in situ stresses (Hight, 2000). Measurements of V_s should also be made with shear wave propagation in the same direction as in the field, with the same plane of polarisation. For this reason, vertically propagated shear waves (V_{Svh}), as typically measured in standard triaxial setups, should be preferably compared with Down-Hole results, as schematically illustrated in Figure 2.17.

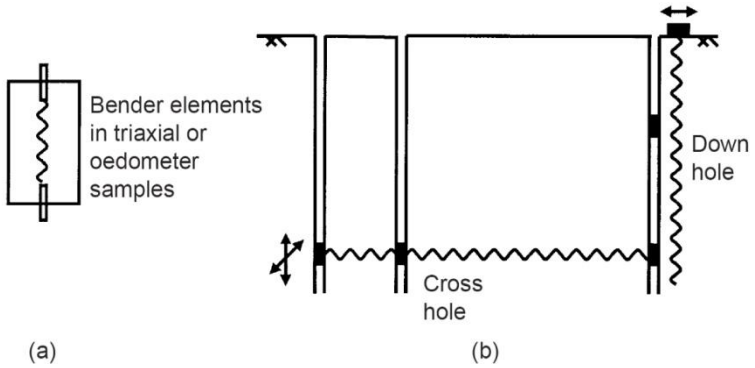

Figure 2.17 - Measurement of G_0 from shear wave velocities in: a) laboratory tests; b) in situ tests (Atkinson, 2000)

2.4.4. COMPARISON OF CYLINDRICAL AND BLOCK SAMPLES MEASUREMENTS OF SHEAR WAVE VELOCITIES

2.4.4.1. Introduction

As explained in the previous chapter, the comparison of laboratory and in-situ measurements of seismic wave velocities is an excellent technique for finding out if the sample suffer damage any damage, during the sampling and transport process in the laboratory. During the process of collecting the sample blocks an attempt was made to measure the shear and compression waves with ultrasonic transducers, but for reasons that will be explained, it was not possible.

Due to the impossibility of measuring seismic waves in-situ, the study has been limited in comparing the shear waves in the sample blocks and in the cylindrical samples (collected from the same blocks of soil) in the laboratory, for checking if the sampling technique ,"presented in chapter 4", caused any disturbance during the laboratory tube sampling.

2.4.4.2. Proposed methodology for the measurement of seismic waves

There are different laboratory apparatuses for measure seismic waves, such as the resonant column, plate transducers and bender element, among others. In this experimental work we used two different devices. In the beginning we used plate transducers to measure the waves directly on the sample block, and then, after the cylindrical samples had been prepared for the triaxial apparatus, we used the bender elements. While we didn't encounter any major problems during the observation and interpretation of the seismic waves using the bender element, we faced several difficulties with the ultrasonic transducers.

Initially, the electronic equipment used included a functional generator, an oscilloscope, two pairs of ultrasonic transducers and a laptop computer in which the data was stored. This setup was not perfect because the impulse created by the ultrasonic transmitter couldn't spread to the interior of the sample,

both because the impulse was too low to be received and also because of high density of the sample. These are probably the same issues that prevented the measuring of seismic waves in situ.

On the second occasion we decided to introduce a craft-made amplifier (University of Waterloo) that increased the power of the signal to 800V, but even then the signal was too low to be received. Figures 2.18 and 2.19 show the equipment used and the schematic of the connections.

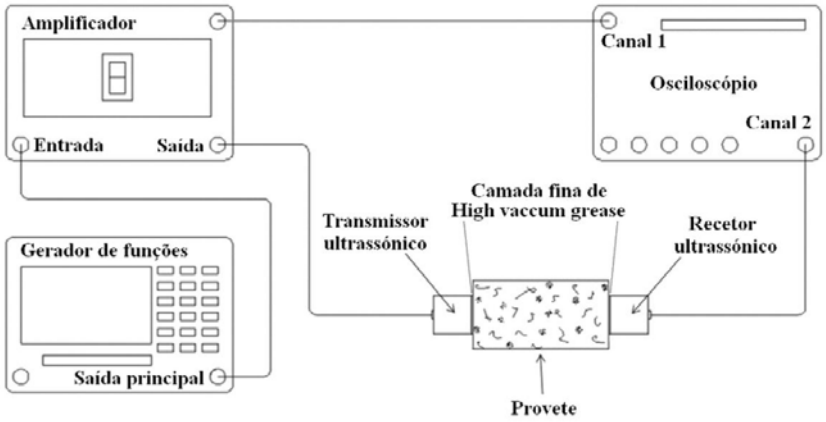

Figure 2.18 – Schematic of the connections employed in the measurement of seismic waves (adapted from Amaral et al., 2012)

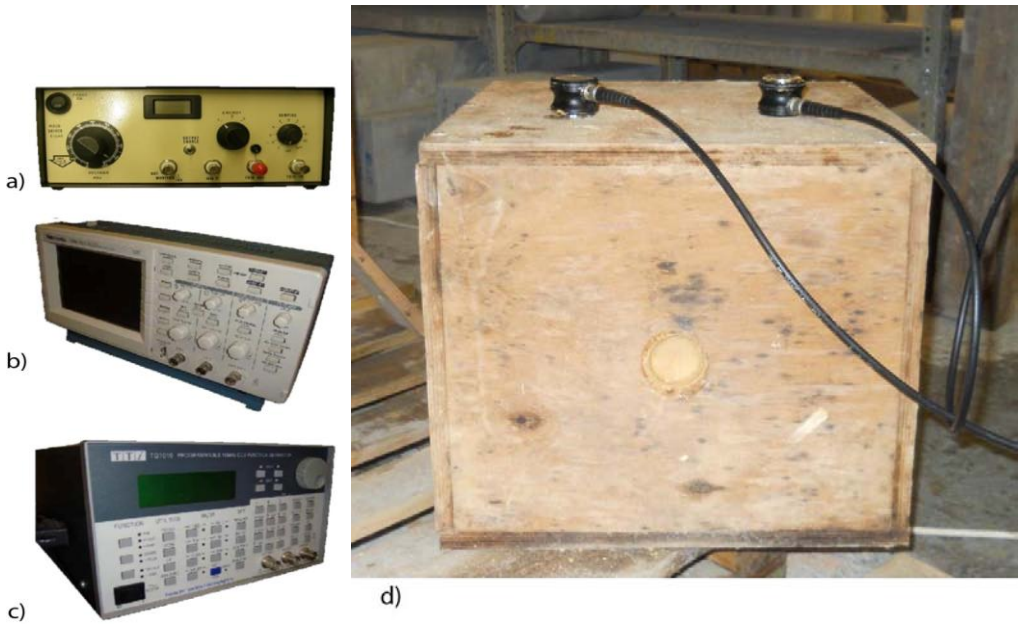

Figure 2.19 – Equipment used: a) Power Amplifier (University of Waterloo); b) Oscilloscope; c) Function Generator; d) Block sample

After testing the ineffectiveness of the classical methods for measuring seismic waves on this sample blocks, a more invasive approach was chosen. We decided to link the compression transducers at the

channel n° 1 of the oscilloscopes, and the share transducers at the channel n° 2, so as to use no more than the function generator and amplifier.

Without the functional generator, the impulse was created by lightly hitting the P-waves transducer with a small hammer, whilst taking care to avoid hitting it too strongly as this could damage the transducer. Using the S-wave transducer as the reciver, it became clear that it was possible, in a certain way, to obtain the velocity of both waves, as both compression and share waves are generated by the hammer strike. The S-waves travel along the whole of the sample block's length to be received by the S-waves transducer at the opposite end of the block, while the P-waves, as the sample block is confined to a wooden box, are reflected and received by the first transducer. Figure 2.20 shows the waves' arrival time and distance travelled.

The results obtained using the test specimens are plausible, as the velocities detected are very close to the scientific litterature. Moreover, the difference in velocity among the different sample blocks is minimal.

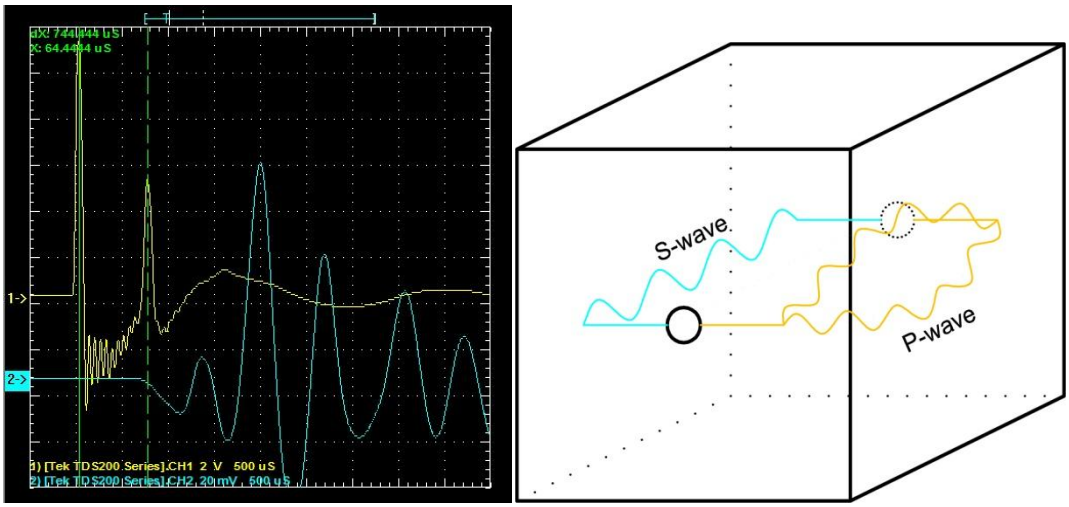

Figure 2.20 – a) example of a register effected in the test with these types of transducers; b) travel distance of shear and compression waves

For a more consistent comparison, the shear wave velocities should be normalized to the respective void ratio. Since the block samples presented very similar void ratio, the normalisation of the shear wave velocities is unnecessary.

The combination of the results from both cylindrical and block specimen can be made by plotting the laboratory V_s values measured in sample block against the corresponding cylindrical soil sample

values, as shown in Figure 2.21. Perfect agreement of laboratory results would fall on the 1:1 line; below this line, the points indicate that cylindrical specimen values are lower than sample block values.

We expected all of the points to appear below the 1:1 line. The slope of the line connecting each point to zero provides an indication of the loss of shear wave velocity, which can be considered a measure of the sample disturbance trimmed from the block. The results obtained are summarised in Table 2.5.

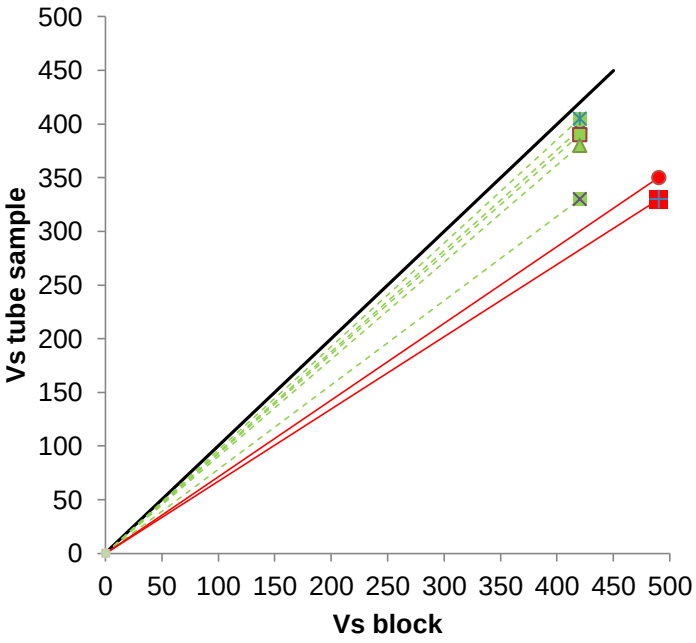

Sample		% loss
Block 7	S-1	6%
	S-2	7%
	S-3	9%
	S-4	22%
	S-5	4%
Block 6	S-A	32%
	S-C	28%

Table 2.5 – Difference between Vs measured in laboratory

Figure 2.21 – Shear wave velocities for all tested specimens

The percentages of loss shown in the table refer to shear wave velocity, but could also be associated with the stiffness or natural structure. The similarity of the V_s trends in the laboratory tests is evident, the figures show that the differences between the shear wave velocities of the two sample blocks are smaller. It can be seen how all the cylindrical specimens show minimal damage, with specimen S-5 being the least disturbed sample, with 4% of loss, and specimen S-A the most disturbed sample, with 32 % of loss. It should be noted that the specimens obtained from sample block 6 are the ones that suffered the most disturbance. A plausible explanation for the values obtained may lie in the fact that the two samples, S-A and S-C, were tested much later than the other samples. As pointed out by Ferreira (2008), ageing during storage is an influential parameter in the shear stiffness of a soil.

Considering the stages of a sample (from sampling, to storage, to preparation, to laboratory testing) shear velocity losses below 15% appear to be minimal and therefore acceptable as an indicator of an

excellent quality sample. A gradual scale can then be empirically and experimentally established: below 30% for a very good quality sample; below 40% for a good sample; below 50% for a fair quality sample. But if above 50% of V_s loss, the quality of the sample is poor and the sample should be considered disturbed, and therefore unsuitable for careful laboratory testing and characterization (Ferreira et al., 2011).

From this plot, it is possible to define different categories of sample quality (or sample disturbance). Ferreira (2008) proposed a classification of sampling quality (or sample condition) based on the comparison of normalised shear wave velocities in the field and in the laboratory, as indicated in Figure 2.22 and Table 2.6.

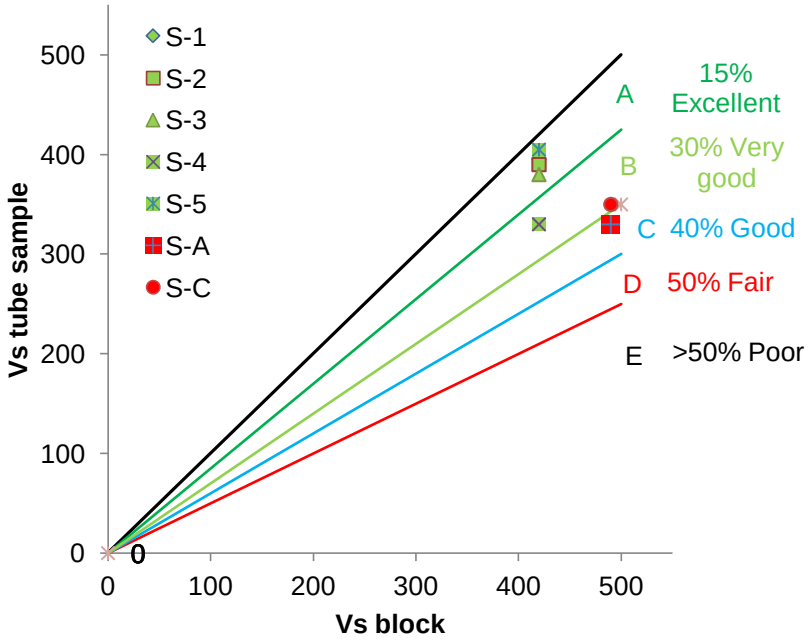

Figure 2.22 – Proposed classification of sampling quality from Ferreira (2008)

Table 2.6 – Proposed classification of sampling quality and sample condition based on the comparison of normalised shear wave velocities in the field and in the laboratory Ferreira (2008)

Quality zone	% loss in V_S	$V_{S\ lab}/V_{S\ in\ situ}$	Sample quality	Sample condition
A	< 15%	< 0.85	Excellent	Perfect
B	15% - 30%	0.85 – 0.70	Very good	Undisturbed
C	30% - 40%	0.70 – 0.60	Good	Fairly undisturbed
D	40% - 50%	0.60 – 0.50	Fair	Fairly disturbed
E	> 50%	> 0.50	Poor	Disturbed

The above mentioned classification are not the only ones present in the literature. Landon et al. (2007) suggested another classification based upon tests on Boston blue clay, however the later classification is less restrictive than the one proposed in Table 2.6.

It should be emphasized that these classifications are based on the comparison of shear wave velocities in the field and in the laboratory, while the study that we conducted is limited to the comparison of shear wave velocities measured solely in the laboratory. It can be concluded that the degree of disturbance suffered during the laboratory tube sampling is minimal, in fact Figure 2.22 shows clearly how nearly all of the specimens fall between the quality levels of excellent and very good.

2.5. SATURATION PROCESS

2.5.1. INTRODUCTION

As pointed out by Head, K.H. (1992), the term "saturation" as a stage of the test refers to way by which the pore water pressure in the specimen is increased so that air as a separate phase in the void spaces is eliminated.

In triaxial compression tests on saturated soils, standard equipment and procedures are readily available for the measurement of pore water pressure, but when dealing with partially saturated soils there is the added complication of the pore air pressure which differs from the pore water pressure. In the majority of effective stress triaxial tests carried out in practice these difficulties are avoided by saturating the specimen as the first stage of a test. There are exceptions in which the achievement of full saturation by the normal procedure is not necessary, or even desirable. However, when the primary purpose of the test is to measure the shear strength at failure in soils that are not initially fully saturated, saturation is normally carried out as a first step.

Before the saturation stage, water was percolated through the sample at an average back pressure of 5 kPa (10 kPa at the bottom platen and 0 kPa at the top platen) and a minimum volume of 500 ml was considered necessary to remove most of the large air bubbles. The differential between applied back pressure and cell pressure should not be greater than the effective consolidation pressure, or 20 kPa, whichever is less, and should not be less than 5 kPa.

Saturation is effected by raising the pore pressure to a level high enough for the water to absorb into a solution all the air that originally occupied the void spaces. At the same time the confining pressure is raised, in order to maintain a small, positive, effective stress on the specimen. There are several ways of doing this, but the most common method in practice is to apply a "back pressure" to the pore fluid incrementally, alternating with increments of confining pressure to ensure that the effective stress remains positive. In this work the samples were saturated in increments of back-pressure of 50 kPa,

generally up to 500 kPa. Once a specimen has been saturated, the elevated pore water pressure should, if possible, be maintained at that level. Reduction of pore pressure below about 150 kPa could lead to the dissolved air coming out of the solution again, in the form of bubbles.

The advantages of using this technique to obtain full saturation are several, the application of back pressure not only dissolves air contained in the specimen, but also eliminates any air bubbles in the drainage line and pore pressure connections which could not be flushed out, moreover any air trapped between the membrane and the specimen is also dissolved.

2.5.2. DIRECT MEASUREMENTS OF THE DEGREE OF SATURATION

Knowledge of degree of saturation, S, is often needed because this characteristic influences such fundamental soil properties as shear strength and compressibility. S is defined as the ratio of the volume of water to the volume of voids in soil and can be expressed in the following form:

$$S = \frac{V_w}{V_v} \tag{2.29}$$

where,

- V_w is the volume of water;
- V_v is the volume of voids.

When all the voids in a soil mass are completely filled with water ($S = 1$), the soil is said to be fully saturated, in this case, the soil is considered a two phase medium having a solid and a liquid phase.

In laboratory tests, S is generally determined using the following equation:

$$S = \frac{W_w}{\gamma_w V_v} = \frac{W_w}{\gamma_w (n \cdot V)} \tag{2.30}$$

where,

- W_w is the weight of water;
- γ_w is the unit weight of water;
- V is the total volume;
- n is the porosity.

The weight of water is determined by measuring the difference in weight between the sample in its moist condition and at oven dry condition (W_s). The total volume is determined measuring the dimensions of samples of simple shapes. In the laboratory this was used to establish the degree of saturation of each specimen at the end of every triaxial test.

It becomes clear, from the data shown in Table 2.7, that every sample, except for S-5 and S-A, obtained a full grade of saturation. It can also be noted that specimens S-1 and S-3 achieved a degree of saturation of more than 100%, which is impossible, but confirms the proposed limits of this methodology which is too heavily influenced by human error.

Table 2.7 – Direct measurements of the degree of saturation

Sample	**W_w** (g)	**V_v** (cm^3)	**S (%)**
S-1	233.44	223.06	1.03
S-2	222.31	223.84	0.97
S-3	238.01	231.93	1.01
S-4	233.44	231.19	0.99
S-5	192.22	209.21	0.90
S-A	203.87	218.93	0.91
S-C	213.94	213.32	0.98

2.5.3. INDIRECT MEASUREMENTS OF THE DEGREE OF SATURATION

Indirect methods of estimating S involve measurements of some other parameters which are highly sensitive to the change in S. Skempton's pore water pressure coefficient B, commonly known as B-value and compression P wave velocity, V_p are two such parameters.

Skempton's B coefficient is a significant pore-fluid parameter, which is defined as the ratio of the induced pore water pressure to the applied total confining stress in undrained conditions. Skempton (1954) demonstrated the relationship between B-value and S based on the theory derived and confirmed the theory using experimental data. The equation derived by Skempton (1954) expressing the B-value is as follows:

$$B = \frac{\Delta u}{\Delta \sigma_3} = \frac{1}{1 + \frac{nC_v}{C_c}} \tag{2.31}$$

where,

- n is the porosity;
- C_c is the compressibility of the soil structure;
- C_v is the compressibility of the pore fluid/air.

Assuming the soil grains to be incompressible, Equation (2.31) provides B = 1 for fully saturated condition, B = 0 for completely dry condition, and a value in-between for partially saturated condition. In reality, however, soil grains are not totally incompressible and may never reach a value of 1 when fully saturated (Bishop 1976). Nevertheless, the B-value is directly related with S and can be easily measured in laboratory triaxial tests (Altun and Goktepe 2006).

As pointed out by Ferreira (2002) conventionally saturation of the specimen is established for value of B equal to 1, accepting however values higher than 0.9 (varying according to the type of soil).

It has long been recognized that compressional waves, in contrast to shear waves, propagate in saturated soils with a velocity that is strongly affected by the water filling the interstices of soil grains. According to Domenico (1974), when water saturation is low, V_p decreases with increasing saturation since the fluid makes the density of samples become larger. However, when water saturation reaches a high value, V_p has an obvious increase.

Some researchers, including Ishihara et al. (2001) and Yang (2002), among others, have attempted to correlate V_p directly to S, while others have considered the B-value as the representative of S and tried to find the relation between V_p and the B-value. This research has also been addressed by Ferreira (2002), proving that while parameter B grows slowly as the total stress increases, the values of the P-wave velocities remain almost constant until the last levels of tension, under which they undergo a sharp rise, rapidly reaching values close to the speed of propagation of sound in water (approximately equal to 1500 m/s).

In this work, the specimens' degree of saturation in triaxial cells was measured through B-value and compression wave's velocity. As shown in the following graphs, there is a mismatch between the methods. Considering Skempton's coefficient, every specimen's saturation is reached under 300 Kpa pressure, while, considering P-waves velocity, saturation takes place with a pressure greater than or equal to 500 Kpa. This test highlights that Skepton's method cannot be universally used as it depends on the type of the soil involved in the measures.

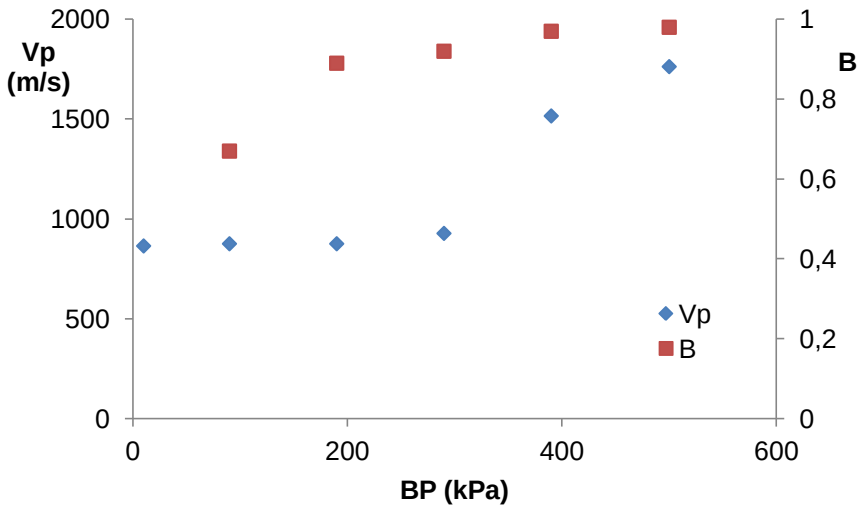

Figure 2.23 – Specimen S-1, relationship between compression wave velocities and B-value under different levels of back pressure

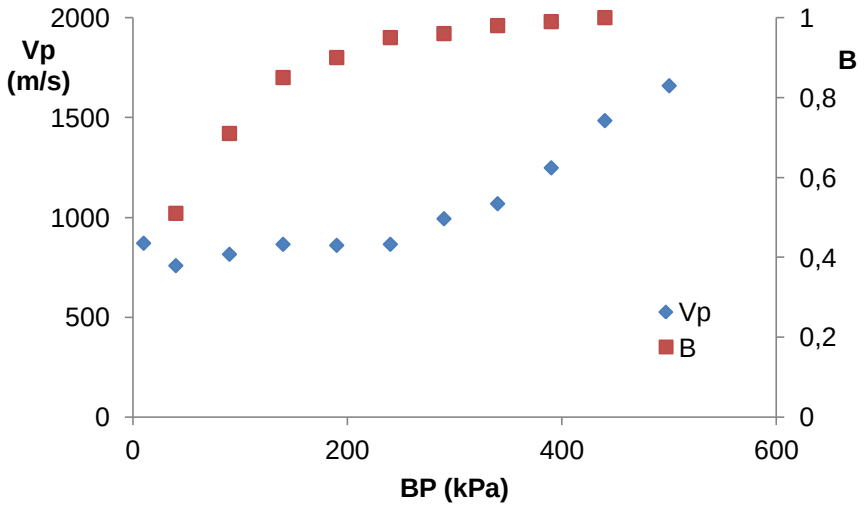

Figure 2.24 – Specimen S-2, relationship between compression wave velocities and B-value under different levels of back pressure

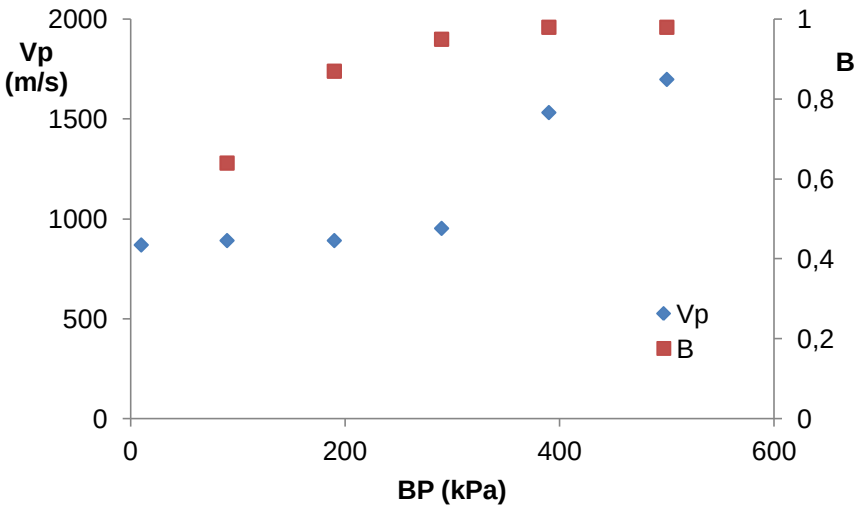

Figure 2.25 – Specimen S-3, relationship between compression wave velocities and B-value under different levels of back pressure

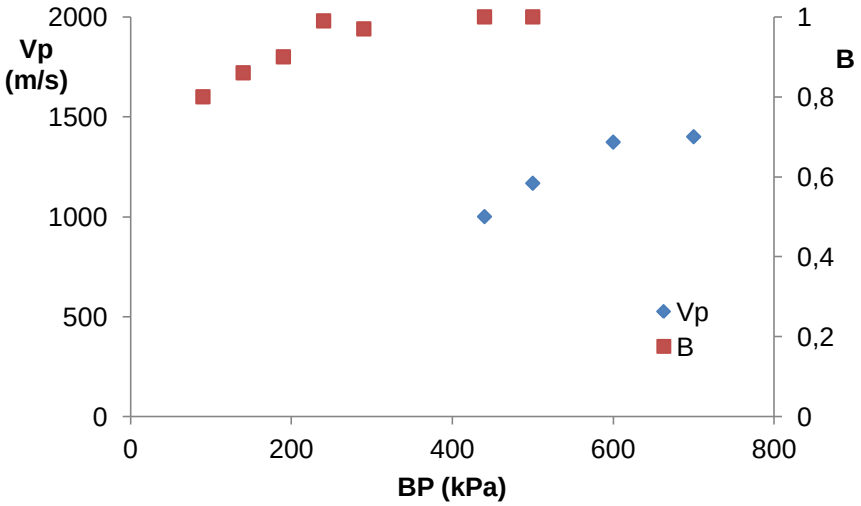

Figure 2.25 – Specimen S-4, relationship between compression wave velocities and B-value under different levels of back pressure

3

GEOTECHNICAL CHARACTERIZATION OF SOILS

3.1. PHYSICAL PROPERTIES

3.1.1. SOIL PARTICLE DENSITY

The particle density of soil (ρS) represents one of the soil's basic physical properties and it depends on the composition of both the mineral and the organic soil components. Particle density focuses on just the soil particles and not the total volume that the soil particles and pore spaces occupy in the soil. The density of soil particles is a result of the chemical composition and structure of the minerals in the soil. See Figure 3.1.

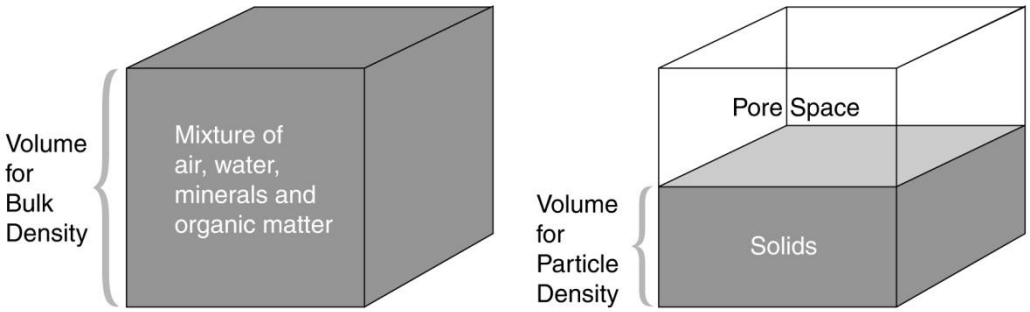

Figure 3.1 – Schematic of volume for bulk density and volume for particle density

Particle density data are used to better understand the physical and chemical properties of the soil. For example, the particle density indicates the relative matter amounts of organic matter and mineral particles in a soil sample. The chemical composition and structure of minerals in a soil sample can be deduced by comparing the soil's particle density to the known densities of minerals such as quartz, feldspar, micas, magnetite, garnet, or zircon.

To calculate soil particle density the mass and volume of only the solid particles in a soil sample must be measured, not the air and water found within the pore spaces between the particles.

This measure is carried out by putting a soil sample in a flask with distilled water, Figure 3.2 shows the soil sample being prepared and put into the flask. The soil/water mixture is boiled to remove all air from the sample. After the mixture has cooled, water is added to the mixture to obtain a specified volume. The mass of this mixture is then measured. The mass of the water is then subtracted from the mass of the soil and water. The particle density is calculated from the mass of the solid particles in a specified volume.

Figure 3.2 – Preparation of 25g soil to be placed into the flask

From the laboratory test carried out for determination of the particle unit weight (□s), it was possible to obtain the data in the Table 2.6.

Table 3.1 - Particle unit weight

Sample	1	2	Media
γ_s (kN/m3)	25.9	26.1	26

As pointed by Viana da Fonseca et al. (1997), typical value of particle unit weight of residual soils from granite in the northwestern part of Portugal are included in the range of 25.6 – 26.7 (kN/m3), according with the data we found. This value been then used to determine void ratio and porosity of soil.

3.1.2. GRAIN SIZE DISTRIBUTION

The standard grain size analysis test determines the relative proportions of different grain sizes as they are distributed among certain size ranges. Residual soils from granite are very frequent in Portugal

where this type of rock is very abundant especially in the north and central region. The grain size distribution of this formation can change within a certain range, as illustrated in chapter 2.

Grain size analysis of the soil tested was performed by mechanical or sieve analysis to determine the distribution of the coarser material, in which the particle sizes are larger than n° 200 (0.075 mm) and smaller than 4 n° (100 mm), while the distribution of particle sizes smaller than 0.075 mm is determined by a sedimentation process, using a hydrometer to secure the necessary data. Summarizing, a weighed sample of material is separated through a series of sieves with progressively smaller openings. Particle size distribution is determined by weighing the material retained on each of the sieves and dividing these weights by the total weight of the sample. The soil passing the 200 sieve is thrown in water and over time the hydrometer will record the various specific gravities of the soil and water mixture. In Figure 3.3 the grain size distribution curves of soil are plotted.

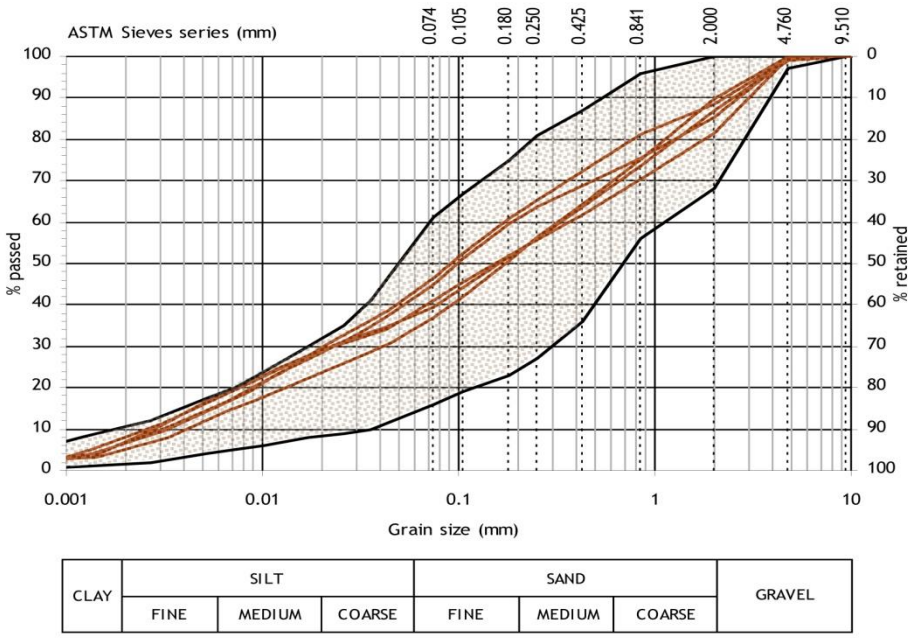

Figure 3.3 – Grain-size distribution curve, framed with the typical grain-size fuse for Porto residual soil

As can be seen, the grain-size distribution curve of the tested soil is well graded, with the predominance of the sand fraction. This soil is classified as a silty sand (SM) according to the unified classification system ASTM.

Figure 3.3 also includes the envelopes of more than one hundred grainsize distribution curves obtained in previous works on residual soil from Porto granite, compiled by Viana da Fonseca (1996). The

results of this experimental site fit well inside these envelopes curves, demonstrating the representativity of this soil as a typical residual soil from Porto granite.

Figure 3.4 – Grain size analysis by sedimentation

3.2. MECHANICAL TESTS

3.2.1. INTRODUCTION OF DIRECT SHEAR TEST

The direct shear test is one of the oldest strength tests for soils. At the Geotechnical Laboratory of FEUP, a direct shear device was used to determine the shear strength of the residual soil (i.e. angle of internal friction and the cohesion). The defects in the apparatus involve the inability of the engineer to control the principal stresses and strains, problems with coarse particles in the shear zone, the fact that the sample doesn't necessarily fail on the weakest surface, which could be inclined to the horizontal. Some of these aspects have been analyzed in more detail in the PhD thesis of Viana da Fonseca (1996).

Direct shear samples are shaped like flat disks or flat rectangular prisms. The size of the sample is partially controlled by the grain size of the soil. For clays, silts, and sands, the sample width is typically 50 to 100 mm, while for soils with larger particle sizes, the width may increases. In our case, all samples were trimmed from Block 7, collected at 5 m depth, in a cylindrical box of dimension 63X 25 mm^3.

As the test progresses, the contact area between the two specimen halves varies with the relative displacement, between the upper and lower shear box. The area correction needs to be applied to both the normal stress and the shear stress. For a typical sample diameter of 63 mm, the error on shear and normal stresses may be 20 % when displacement is 1 cm (Bardet, 1997), so it is important to make the appropriate correction.

In order to obtain mechanical properties of the samples collected from block 7, were carried out 3 direct shear tests with different values of normal stress of 25 kPa, 50 kPa and 100kPa. Figure 3. 5 illustrate two details of samples preparation for the direct shear test.

Figure 3.5 – Details of direct shear test: a) Specimen preparation; b) Sample positioned inside the shear box.

3.2.2. INTERPRETATION OF RESULTS

The material through which tests were carried out have a good quality, since the peak value is well visible in most of the graphics. From the plot of the shear stress versus the horizontal displacement for each test, it is possible to obtain the curves, for three different stress, as shown in Figure 3.6. Moreover, plotting the horizontal displacement versus the vertical displacement is also possible to determine the angle of dilation in each test.

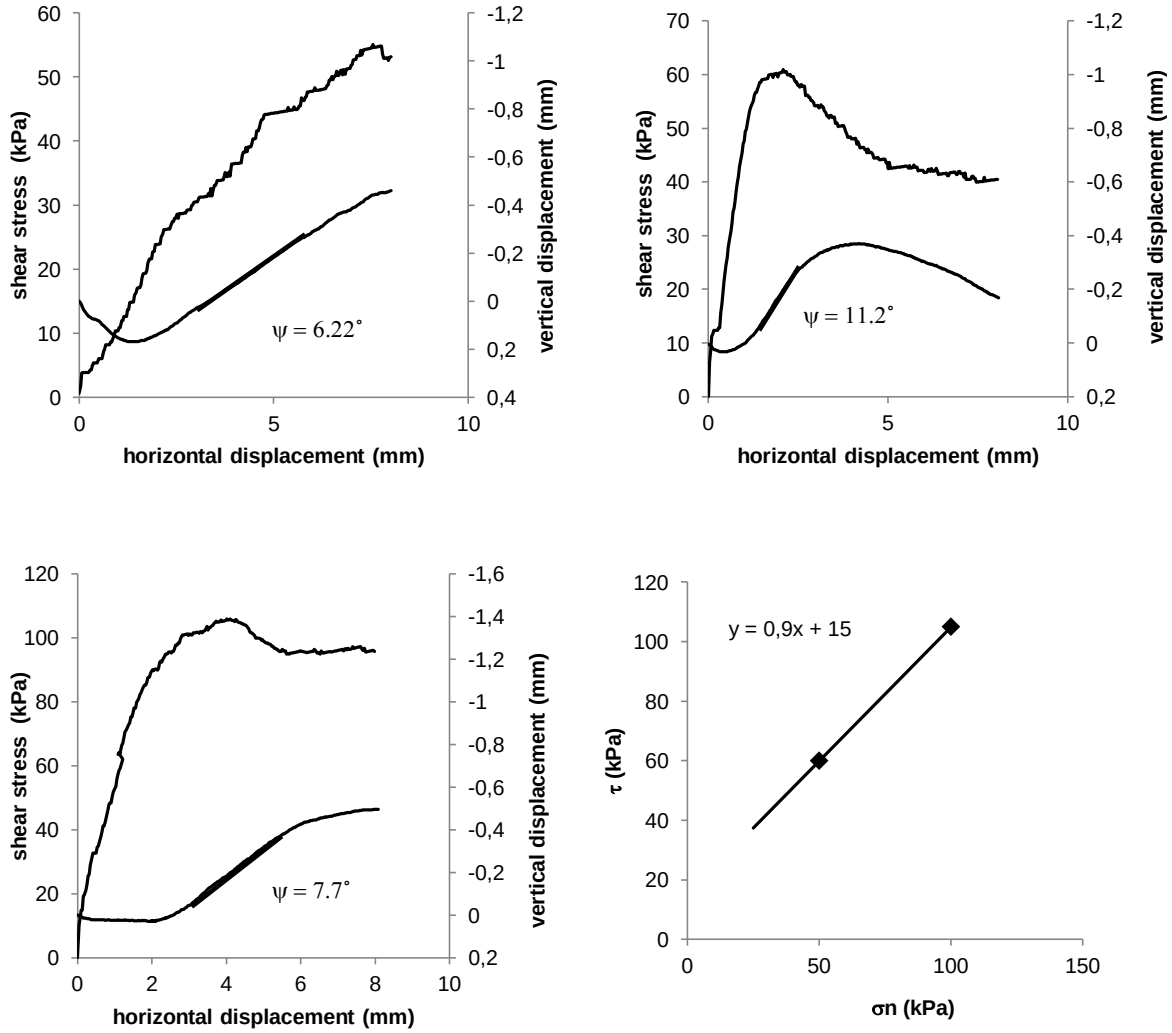

Figure 3.6 – Direct shear test data: a) σ_n=25 kPa; b) σ_n=50 kPa; c) σ_n=100 kPa; d) Strenght envelope from direct shear test

Using a Mohr-Coulomb strength model, and plotting the values corresponding to the ultimate stress on the plane $\sigma - \tau$, it was found the angle of friction at constant volume, as shown in Figure 3.6d. We can see how the test, carried out with a 25 kPa σ_n, has an anomalous behavior because the peak value is not reached like in other tests. Therefore peak angle and cohesion found by these two values, could be unclear, $\varphi' = 42$ and $c' = 15$ kPa.

In spite of these uncertainties, identified parameters are similar to the typical residual soil values. To obtain the costant volume friction angle, the box share test guide has been switched on in the revers direction, so that we get the ultimate strenght value for each stress value applayed.

For example, in Figure 3.7, are shown curves obtaind from "horizontal displacement" versus "share stress", which are related to the different steps during the test with a nromal stress of 50 kPa.

After failure stress is attained, the resisting shear stress gradually decreases as shear displacement increases until it finally reaches a constant value called the ultimate shear strength.

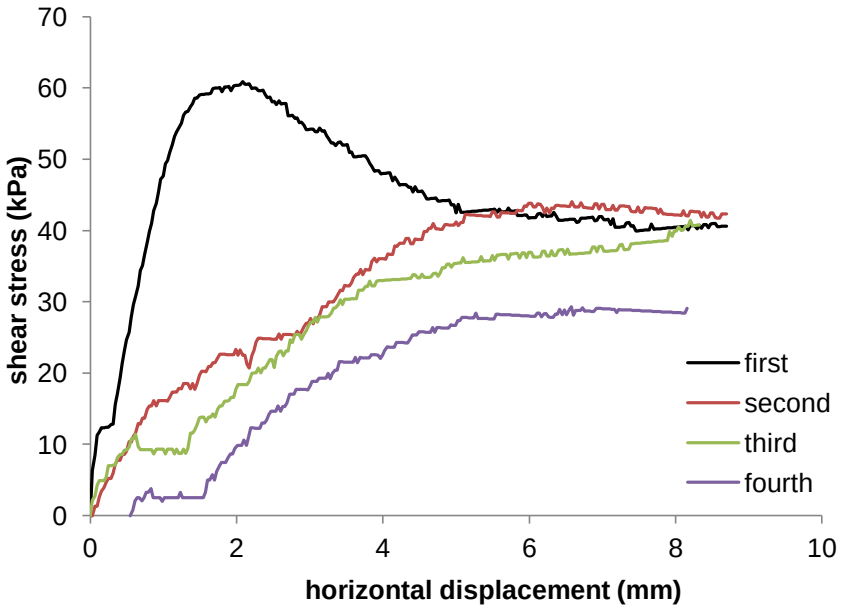

Figure 3.7 – Direct shear test data

Average values reached in each test, are reported in the $\sigma - \tau$ plan, from which we obtain the plot in Figure 3.7. The straight line is obtained interpolating the three values in the plot, forcing it to pass through the origin. In this way we obtain a null cohesion and angle of friction at constant volume is equal to 36.5°.

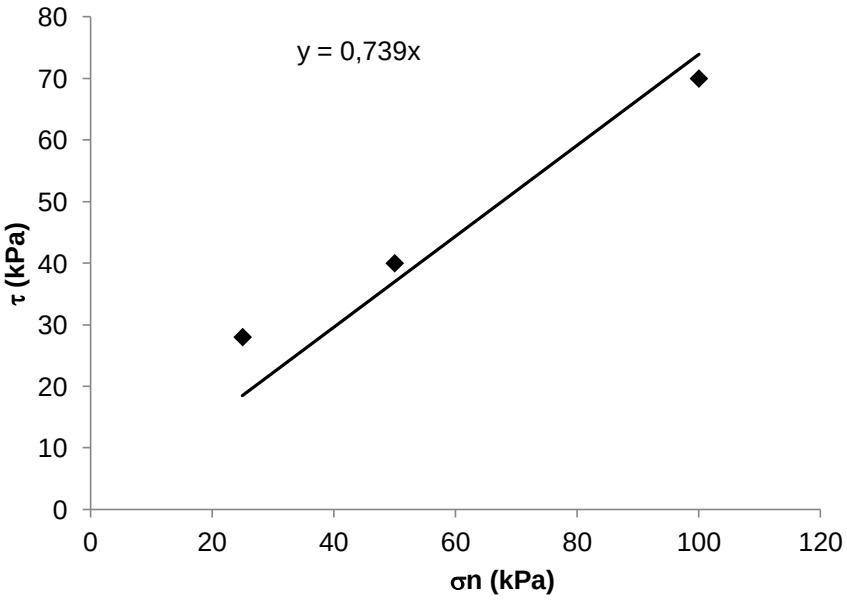

Figure 3.8 – Strenght envelop from direct shear test

However, several publications (Jewell 1989, Mitachi & Tamate 1997, Stoewahse 2001, Goldscheider 2003, Lindemann 2003) have shown that various aspects, e.g. the assembly of the upper box and therewith connected wall friction effects, influence the results of direct shear tests. Jewell (1989), notes that the value of friction angle can be overestimated due to the confinement produced by the shear box, increase in the order of 5%. This issue has also been addressed in residual soils from Porto by Viana da Fonseca (1996). For these reasons the angle of friction we found could be slightly overstimated.

Many authors suggest a relationship between the plane strain angle of friction and the angle of dilation in the soil, as in the case of Bolton (1986):

$$\phi_p = \phi_{cv} + 0.8\psi \tag{3.1}$$

Replacing equation 3.1 in the Mohr-Coulomb criterion "$\tau = c + \sigma \tan(\varphi)$" is possible to reach the coesion for the tests carried out with a $\sigma_n = 50$ e 100 kPa. In table are summarized the results of the direct share test.

Table 3.2 – Result of the direct shear test

Test	τ_{cv} (kPa)	φ_{cv}	τ_p (kPa)	$C_{bolt.}$(kPa)
Block 7- σ_n=25 kPa	28	36.5	//	//
Block 7- σ_n=50 kPa	40	36.5	60	10
Block 7- σ_n=100 kPa	70	36.5	105	20

3.2.3. TRIAXIAL TESTING APPARATUSES

Early devices with many of the characteristics of current triaxial devices were originated by Buisman (1924) and Hveem (1934) according to Endersby (1950) but the first devices that resembled modern equipment were developed in the early 1930's by Casagrande at Harvard and Rendulic in Vienna, both apparently under the direction of Terzaghi.

The Triaxial Compression Test is a laboratory test method that is used to assess the mechanical properties of soil or rocks. A cylindrical specimen of soil is encased in an impervious membrane is subjected to a confining pressure and then loaded axially to failure in compression. This test is performed to simulate in situ confining pressures to observe the soil response under conditions that may approximate those in situ.

Primary parameters obtained from the test may include the angle of shearing resistance φ', cohesion c', and undrained shear strength c_u, and others parameters such as the shear stiffness G that may also be determined.

There are three primary triaxial tests conducted in the laboratory, each allowing the soil response for different engineering applications to be observed. These are:

- Unconsolidated Undrained test (UU)
- Consolidated Undrained test (CU)
- Consolidated Drained test (CD)

In this work all the specimen were tested with the consolidated drained test, using two different devices which will be described in the next section.

CD test is comparatively slower than others for this reason it requires more time than other methods. In this test soil consolidation occurs under normal load and drainage is allowed during the consolidation. At the completion of the consolidation process, the drainage conditions are to be allowed while normal stress is increased at such a rate that no pore pressure is developed. Thus the resulting parameters of the shear strength are in terms of effective stresses.

3.2.2.1. Triaxial apparatus – FEUP

Low pressure triaxial tests were performed at the Geotechnical Laboratory of FEUP. From low pressures it is intended that the maximum cell pressure that can be achieved in those cells is 1700 kPa. Two types of different apparatus were used, which will be described in the following sections.

3.2.2.1.a). Conventional triaxial cell with bender elements

This apparatus is a conventional triaxial cell that was adapted to include T shape bender/extender elements (Ferreira, 2008). It is equipped with Hall Effect transducers (Clayton et al., 1989) that enable axial and radial local deformation measurements. Figure 3.9 shows the general setup of the equipment (a), the T shape bender/extender elements (b) and the Hall Effect transducers (c). For the present program of tests an internal load cell of 5 kN of capacity was used. The dimensions of the specimens tested in this apparatus were 70 mm of diameter and 140 mm high.

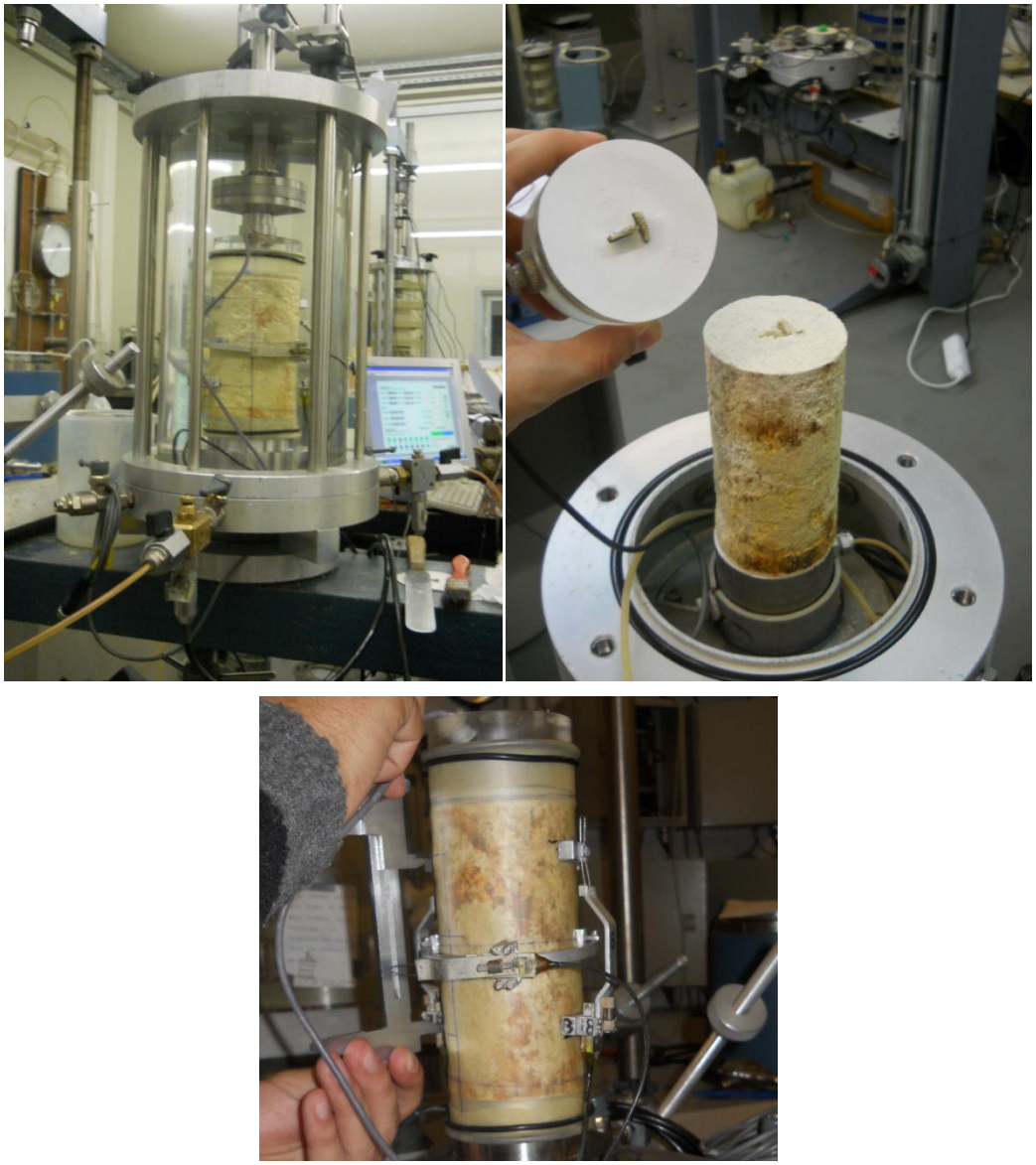

Figure 3.9 – Conventional triaxial cell with BE: a) setup; b) top cap with bender/extender elements; c) axial and radial Hall Effect transducers

3.2.2.1.b). Bishop-Wesley stress-path cell

One of the Bishop-Wesley stress-path cells available at the Geotechnical Laboratory of FEUP enables testing 70 mm and 100 mm diameter specimens. In these systems the axial strain is applied hydraulically using computer controlled stepper motors or motorised Bishop rams and thus it does not require a separate load frame. Both cell and pore pressures are computer controlled through TRIAXÒ software.

The apparatus can carry out routine strain controlled triaxial tests or tests in which the axial stress is controlled and it can change from stress control to strain control during a test with little disturbance.

The cells are equipped with standard transducers for the measurement of strain, pore pressure and volume change as well as an internal load cell. The internal load cells were chosen for each set of tests depending on the expected peak strength of the soil. The tests were performed only with LDT's for local axial deformation measurements (Figure 5.11b).

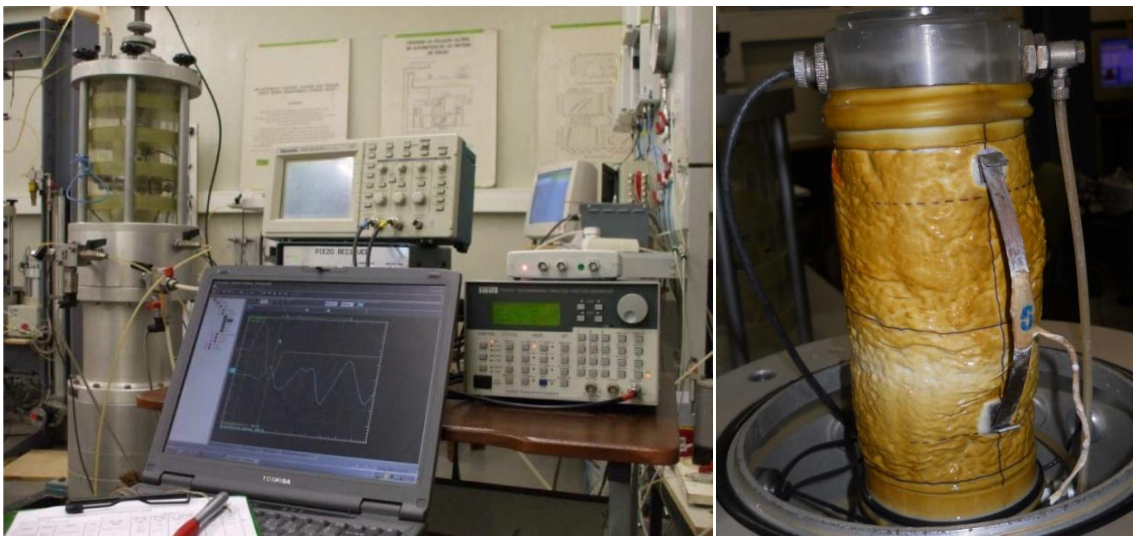

Figure 3.10 - Bishop Wesley stress-path cell: a) setup; b) specimen with LDT's

3.2.2.2. Preparation of cylindrical samples

The natural samples used in this research were taken from the sample block. The block samples were trimmed in order to produce cylindrical specimens for testing in the standard triaxial and stress-path apparatuses.

The preparation of these cylindrical samples consists in trimming this shape with the use of a guiding mould, typically an aluminum liner with a vertical cut. In this way, pulling he mould, soil can enter it in as shown in Figure 3.11.

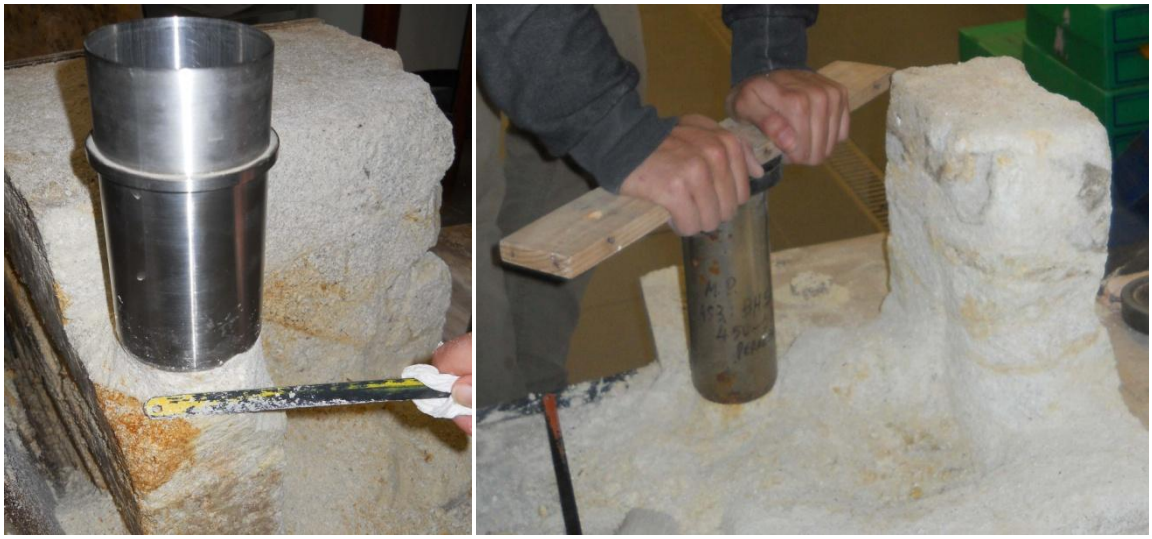

Figure 3.11 – Trimming of cylindrical 70 diameter samples for standard triaxial testing from block samples B 7

Following the sample preparation procedure, this specimen has been pulled out by a hydraulic press, then a thin rubber membrane was stretched and placed around the sample for installation in the testing apparatus. Since these samples were tested using top and bottom BE, the position of these transducers was defined. The BE slots were marked, to ensure proper contact and to remove any grains that could compromise coupling or even break the transducers.

3.2.2.3. Testing ptogram and results

As already said in the previous chapter, the consolidate drenate triaxal test, have a main role in this disertation. First, we realized several triaxial test, to obtain the classic strength and strain parameters of tested material. Specimens used in triaxial tests have been collected from block 6 and 7, considering that every sample block have been collected 5 meters deep, where we found a total vertical stress of about 100 kPa. Every test has been realized assuming a coefficient of earth pressure at rest $k_0 = 0{,}5$.

Totally, specimens tested have been 7: S-1, S-2, S-3, S-4, S-5 from sample block 7 and S-A, S-C from sample block 6.

Following its preparation, each sample was set-up in the respective testing device. Special attention was given to the installation and coupling of the BE with the soil, in order to guarantee the best possible transmission of the seismic waves.

Taking into consideration the sensitive nature of the structure of this soil and also the purpose of assessing sample disturbance, the reconsolidation technique is particularly influential, as pointed out

by Lo Presti et al. (1999). These authorsdistinguished between wet and dry setting, showing that the dry setting is preferable to the conventional setting method.

In this case, reconsolidation, in most of the specimens, has been reached with wet setting, only S-5 has been reconsolidate by dry seting, however results were the same. Tabella 3.3 riassume i risultati ottenuti nelle prove triassiali.

Table 3.3 – Result of the triaxial test

Soil type	Specimen	B. sample	σ'_{v0}	σ'_{h0}	q_{max} (kPa)	E_0 (Mpa)
Res. soil	S-1	7	100	50	301	17.2
Res. Soil	S-2	7	100	50	116	14.1
Res. Soil	S-3	7	100	50	83	16.2
Res. Soil	S-4	7	100	50	//	53.9
Res. Soil	S-5	7	100	50	425	114.7
Res. Soil	S-A	6	100	50	1427	223
Res. soil	S-C	6	100	50	340	136.2

4

STIFFNESS MEASUREMENTS USING STATIC AND DYNAMIC METHODS

4.1. INTRODUCTION

The rapid development of computing power and of numerical modelling software over the past 40 years has made sophisticated analysis of geotechnical problems accessible to most engineering practices. Typically, computer packages now offer a wide range of constitutive models, which the design engineer needs to choose among, and then obtain parameters for. For structures designed to be far from failure, for example supporting urban excavations, strains in the ground are small. A sound knowledge of stiffness parameters at small strain is essential, if realistic predictions of the ground movements that may affect adjacent buildings or underlying infrastructure are to be made. Methods of determining the stiffness parameters have already been mentioned in previous chapters, following will be presented the results of these tests.

4.1.1 CONSTITUTIVE FRAMEWORKS FOR STIFFNESS

The stiffness of a body (or structure) is defined as the resistance of that body to deformation under applied force. It is derived from:

- the shape of the body
- boundary conditions, such as fixities and load positions
- the stiffness properties of the constituent materials (Young's moduli, etc.).

The recognition of linear load/deformation behaviour is widely attributed to Hooke (1676). In his treatise Hooke recognised elastic behaviour, that is, the behaviour of a material that returns to its original shape after loading is removed.

In reality, according to Bell (1989), Hooke's measurements on long iron wires were too insensitive to show linearity. As early as 1687 James Bernoulli produced data for the gut string of a lute that suggested a parabolic relationship between load and deformation at small strains (although Leibnitz assumed his data were hyperbolic). Over 100 years later, in about 1810, two independent sets of experiments, by Duleau and by Dupin, led to conflicting conclusions. Duleau (1820), testing forged iron for a bridge over the Dordogne river, found linear behaviour at small strain. Dupin (1815), testing wooden beams for ships, found a non-linear response.

The dilemma of Leibniz in the 17th century over the apparently conflicting experiments of Hooke and James Bernoulli has been resolved in favor of the latter. The experiments of 280 years have demonstrated amply for every solid substance examined with sufficient care, that the strain resulting from small applied stress is not a linear function thereof.

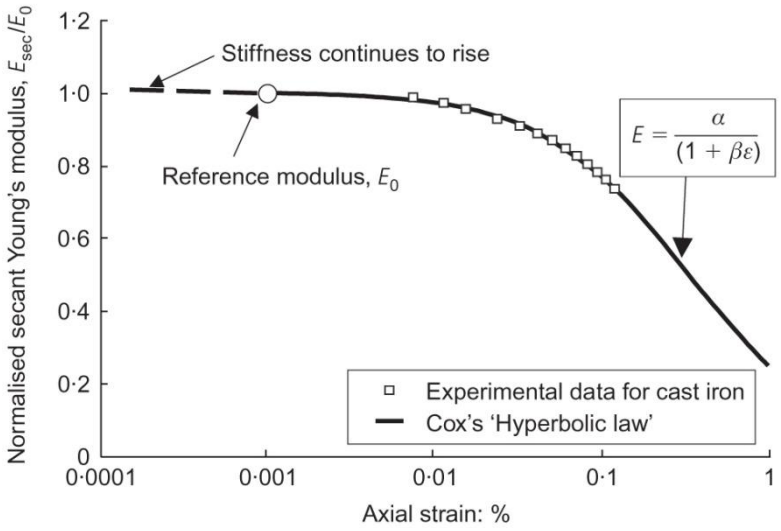

Figure 4.1 – Normalised stiffness data for cast iron (Royal Commission on Application of Iron to Railway Structures, 1849; Cox, 1856)

4.1.2. APPLICATION IN GEOTECHNICAL ENGINEERING

Probably the most commonly assumed behaviour in practical geomechanics is that of isotropic linear elasticity. Characterisation of an isotropic elastic solid requires the determination of only two material parameters (from four possible measurements, i.e. Young's modulus E and Poisson's ratio υ, or shear modulus G and bulk modulus K) for calculations of strain or deformation, and therefore an assumption of isotropic elasticity has the merit of simplicity. However, as noted by Bishop & Hight (1977), there are many reasons to believe that the ground will generally be anisotropic, or at least transversely isotropic.

In the past couple of decades, it has been recognized that the so-called 'elastic' stressstrain response of practically all soils and soft rocks is in fact highly non-linear. This has led to the development of methods of foundation analysis and settlement/deformation prediction that take this into account, such that stiffness non-linearity is now routinely incorporated into many standard computer codes. These achievements have been paralleled by developments in both in situ and laboratory testing methods that allow the details of the stress-strain response to be examined, even at strains as low as 10^{-6}.

Figure 4.1 illustrates a typical stiffness-strain curve for soil and includes typical ranges of strain for laboratory testing and for structures. At small strains the stiffness is relatively large; at strains close to failure the stiffness is small: this is soil being non-linear (Atkinson, 2000). The ranges of strain for the different testing techniques in the figure are similar to those given by Atkinson and Sallfors (1991), while the typical strain ranges for structures are those given by Mair (1993). A typical characteristic strain in the ground is 0.1%; this represents a movement of 10 mm across a gauge length of 10 m (Atkinson, 2000).

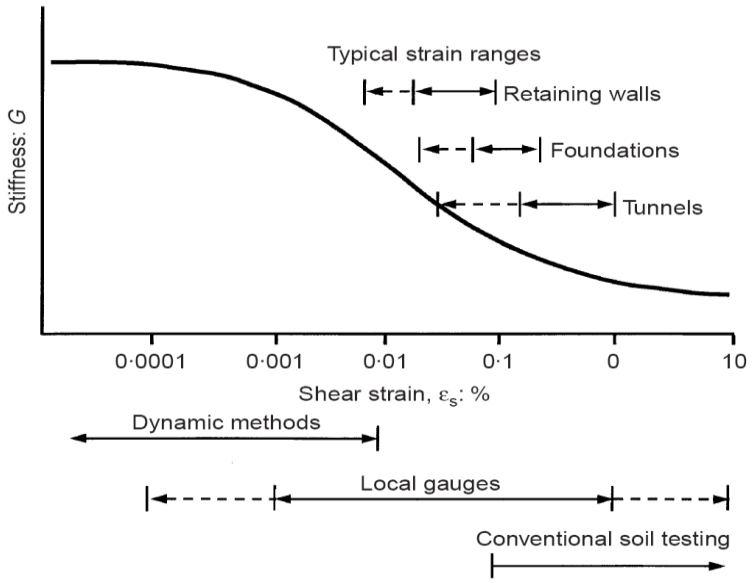

Figure 4.3 - Non-linear characteristic stiffness-strain 65ehavior of soil (after Atkinson and Sallfors, 1991)

Measurement of seismic wave velocities is a practical, non-destructive, frequently non-invasive, cost-effective means of determining small-strain stiffness of soils. Given the particulate nature of soils, wave techniques present unique advantages to study geomaterials without affecting fabric or structural equilibrium and inherent mechanical properties (Fam and Santamarina, 1995). New demands in civil engineering require advanced characterization techniques to assess in-situ conditions and to monitor

processes. Challenges include aging infrastructure, construction in critical/sensitive zones, restrictions created by the urban environment, trenchless construction, installation of new infrastructures, environmental demands and protection. Near-surface geophysical methods can play a critical role in satisfying these needs (Stokoe and Santamarina, 2000).

4.2. STIFFNESS MEASUREMENTS IN TRIAXIAL CELL

4.2.1. INTRODUCTION

Most of the standard triaxial tests carried out in this research included a shearing stage for the characterisation of the strength parameters of the soil samples.

The measurement of soil stiffness at small and very small strains has been carried out under both dynamic and continuous loading in the triaxial apparatus up to high stresses. A system of LDT and Hall Effect transducers has been used to measure axial strain locally during contionuous loading while dynamic stiffnesses were measured using bender elements.

4.2.2. INTERNAL VERSUS EXTERNAL STRAIN MEASUREMENTS

Before presenting the results, it is important to address the observed differences between internal (or local) and external measurements of strain. The example in Figure 4.3 refers to sample S-1. In this test, two LDT were used, directly fixed to opposite sides of the sample. The results presented in the figure clearly illustrate that the externally-measured strain is systematically larger than the internally-measured, particularly at small strains.

For this reason, the calculation of the secant stiffness at small and medium strains was made considering the average of the two internal strain measurements. In cases where the strain level exceeded the limit of the internal transducers, namely the LDT beyond 10% strain, external measurements were used.

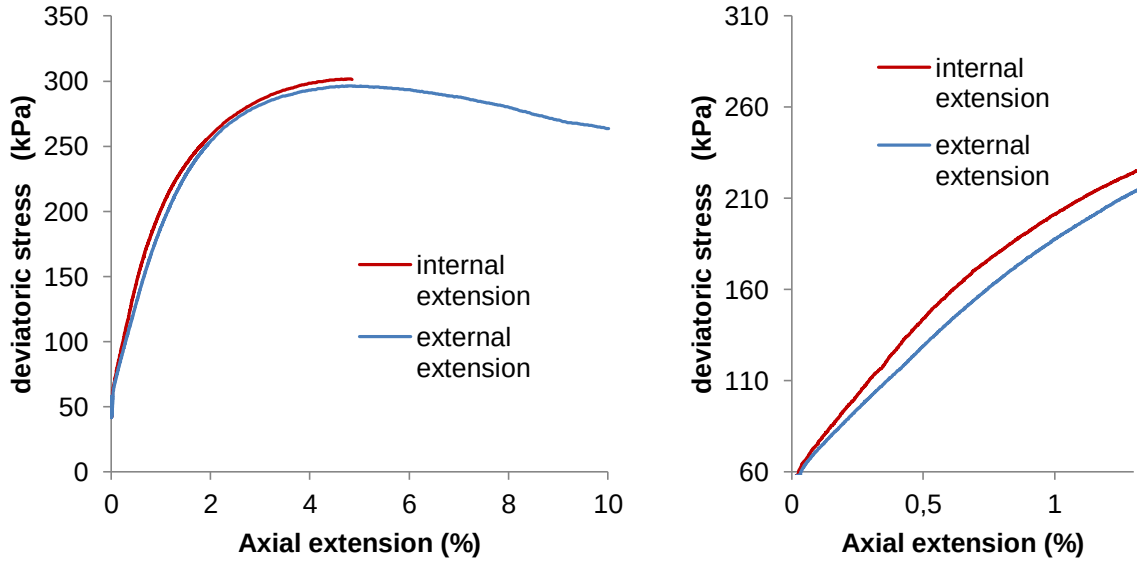

Figure 4.3 – Example of internal and external strain measurements

4.2.3. COMPARISON BETWEEN YOUNG MODULUS MEASURED USING DYNAMIC AND CONTINUOUS LOADING

As to the definition of the different result parameters we begin with the axial stress σ_a, which is defined as:

$$\sigma_a = \frac{F}{A} \tag{4.1}$$

where,

- F is the axial force acting on the specimen;
- A is the specimen cross section area.

The (effective) deviatoric stress is defined as:

$$\sigma_{dev} = \sigma_a - \sigma_r \tag{4.2}$$

The average value of the two axial displacement measurements on opposite sides of the specimen is used for the axial strain calculation. The recorded deformation δ local represents a local axial displacement between the points approximately at ¼ and ¾ of the specimen height. The axial strain is defined as:

$$\varepsilon_a = \delta_{loc}/L_{loc} \tag{4.3}$$

where L_{loc} is the height of the transducer.

The internal (and, if necessary, external) strain measurements can be used to determine the stiffness of the soil. Since in most tests only vertical internal strain transducers were used, the derived stiffness corresponds to the Young's modulus is defined as:

$$E = \frac{\Delta(\sigma_1 - \sigma_3)}{\Delta\varepsilon_a} \tag{4.4}$$

The stiffness can be defined as either secant or tangent. In this work, only the secant stiffness was used, which can be determined from the ratio of the difference in stress and strain from the start of the shearing phase.

The stiffness-strain response can be analysed considering the evolution of the vertical secant stiffness with the measured local axial strain, illustrated in Figure 4.4. For Laboratory Test Results simplicity, in this representation, the strains are indicated as percentage, since that is the usual notation in standard triaxial testing.

Also included in the figure are the estimates of E_0 derived from the shear modulus determined by BE measurements at the final consolidation stage, immediately before the start of the shearing stage. These estimates were computed assuming that a good approximation of the vertical Young's modulus can be obtained from the following equation:

$$E_0 = 2(1 + \upsilon)G_0 \tag{4.5}$$

and assuming a value for the Poisson's ratio υ equal to 0.30, as previously adopted by other authors to characterise this soil (Viana da Fonseca, 1996). In accordance with several authors, the strain at which this elastic moduli was determined in the BE measurements, was considered equal to 3×10^{-6}.

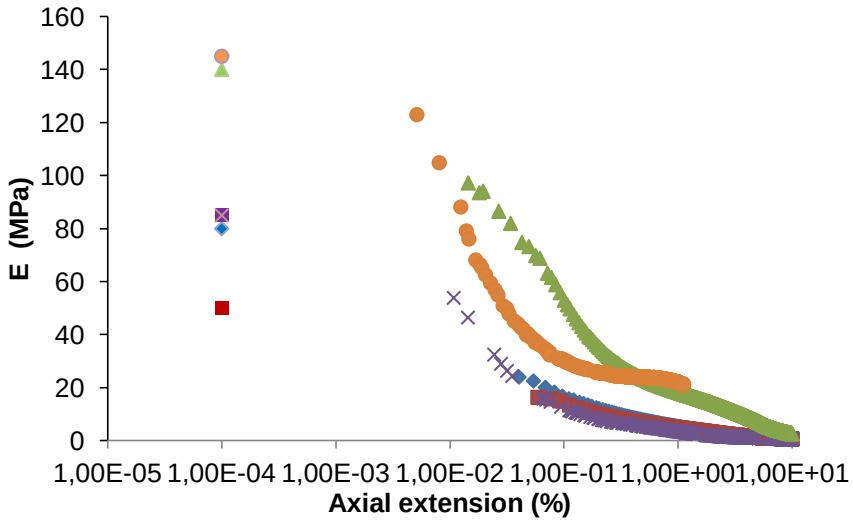

Figure 4.4 - Summary of the stiffness-strain curves, including the estimate of E_0 from BE measurements

From the figure, it can be concluded that there is not a direct correspondence between the relative positions of the dynamic elastic stiffness E_0 and the stiffness degradation curve of the tested samples. One of the reasons for this uncertainty can be associated with the behaviour of the soil, which were not explored in this study. Nevertheless, this plot provides a clear indication of the reduction of stiffness with increasingly larger strains.

CONCLUSION

The use of seismic wave velocities is undoubtedly an optimal method for the measurement of stiffness moduli and for the derivation of a series of relevant soil properties and parameters.

In the laboratory, the most widely-used method for determining V_S is the bender element method. The applications of bender element results are numerous, including the definition of the elastic stiffness parameters, assessment of sampling quality, assessment of anisotropy and process monitoring of saturation.

While the potential and benefit of bender element testing is clear, the interpretation of its results, unfortunately, is not as straightforward, particularly if only one interpretation method is used. In an attempt to overcome this important limitation, a new interpretation framework combining time and frequency domain BE measurements has been proposed and its application effectively reduced the uncertainty and subjectivity often associated with BE testing.

Moreover, seismic wave velocities in soils are influenced by a number of factors, such as the stress state, void ratio, structure, inherent anisotropy, among others, and it is important to be able to isolate each of these factors in order to avoid serious errors.

It is clear that much remains to be investigated and understood so as to minimize the uncertainties existing in the use of seismic waves.

References

Achenbach J.D. (1984). Wave propagation in elastic solids, North-Holland, Amsterdam, Netherlands

Atkinson, J.H. (2000). Non-linear soil stiffness in routine design. Géotechnique.

Amaral, M. (2009). Evaluation of dynamic distortion modulus in soil-cement mixtures by pulse ultrasonic methods in the time domain and resonant modes by spectral analysis of Fourier series. MSc dissertation, Faculty of Engineering of the University of Porto (in Portuguese).

Amaral, M., Rios, S. and Viana da Fonseca, A. (2011). Yielding in isotropic compression of Porto silty sand. (submitted to ACTA Geotechnica Slovenica)

Atkinson, J.H. (2000). Non-linear soil stiffness in routine design. Géotechnique.

Atkinson, J. H. (2008). The Mechanics of Soils and Foundations, Taylor and Francis.

Bolton, M. D. (1986). The strength and dilatancy of sands. Géotechnique.

Ferreira, C. (2008). The Use of Seismic Wave Velocities in the Measurement of Stiffness of a Residual Soil, PhD dissertation presented in the University of Porto.

Ferreira, C., Viana da Fonseca, A. and Nash, D. (2011). Shear Wave Velocities for Sample Quality Assessment on a Residual Soil. Soils and Foundations.

Fioravante, V.; Jamiolkowski, M.; Lo Presti, D.C.F.; Manfredini, G.; Pedroni, S. (1998). Assessment of the coefficient of the earth pressure at rest from shear wave velocity measurements. Géotechnique.

Foti, S.; Lancellotta, R. (2004) Soil porosity from seismic velocities, Géotechnique.

Graham, J. and Houlsby, G. T. (1983). Anisotropic elasticity of a natural clay.

Head, K.H. (1985). Manual of soil laboratory testing. Vol.III - Effective stress tests. Pentech Press, London.

Lee, J. S. and Santamarina, C., 2005, Bender Elements: Performance and Signal Interpretation, Journal of Geotechnical and Geoenvironmental Engineering

Lee, J.-S. ; Santamarina, J.C. (2005) Bender elements: performance and signal interpretation, ASCE Journal of Geotechnical and Geoenvironmental Engineering

Topa Gomes (2009). Elliptic shafts by the sequential vertical excavation method. The Porto metro case study. PhD dissertation presented to the Faculty of Engineering of the University of Porto (in Portuguese)

Viana da Fonseca, A. (1988). Geotechnical characterization of a Porto residual soil from granite. Dissertation presented to the faculty of Engineering of the University of Porto to obtain the Master Degree in Structural Engineering (Report 130/88, NGR, LNEC, Lisboa) In Portuguese.

Viana da Fonseca, A. (1996) Geomechanics of Porto residual soil from granite. Project criteria for direct foundations. PhD Thesis. Porto University, In Portuguese

Viana da Fonseca, A. (2003). Characterizing and deriving engineering properties of a saprolitic soil from granite, in Porto. Characterization and Engineering Properties of Natural Soils.

Viana da Fonseca, A., Matos Fernandes, M. and Silva Cardoso, A. (1997). Interpretation of a footing load test on a saprolitic soil from granite.

Viana da Fonseca, A., Ferreira, C., and Fahey, M. (2009). A Framework Interpreting Bender Element Tests, Combining Time-Domain and Frequency-Domain Methods.